

A unified framework for multivariate two-sample and k -sample kernel-based quadratic distance goodness-of-fit tests

Marianthi Markatou[✉] and Giovanni Saraceno[†]

Department of Biostatistics, University at Buffalo, Kimball Tower,
Buffalo, NY, 14214, USA

Abstract

In the statistical literature, as well as in artificial intelligence and machine learning, measures of discrepancy between two probability distributions are largely used to develop measures of goodness-of-fit. We concentrate on quadratic distances, which depend on a non-negative definite kernel. We propose a unified framework for the study of two-sample and k -sample goodness of fit tests based on the concept of matrix distance. We provide a succinct review of the goodness of fit literature related to the use of distance measures, and specifically to quadratic distances. We show that the quadratic distance kernel-based two-sample test has the same functional form with the maximum mean discrepancy test. We develop tests for the k -sample scenario, where the two-sample problem is a special case. We derive their asymptotic distribution under the null hypothesis and discuss computational aspects of the test procedures. We assess their performance, in terms of level and power, via extensive simulations and a real data example. The proposed framework is implemented in the `QuadratIK` package, available in both R and Python environments.

Keywords: Goodness of fit, Kernel-based tests, k -sample test, Matrix distance, Tuning parameter selection.

1 Introduction

The Goodness-of-Fit (GoF) problem has a long history in statistics, with a significant body of literature dedicated to univariate GoF testing. However, relatively less attention has been given to the two-sample and k -sample problem in the multivariate case. These GoF problems are particularly relevant in modern data analysis, where high-dimensional settings pose unique challenges.

Extensions of univariate two-sample GoF tests in high-dimensional, multivariate settings, utilize graph-based multivariate ranking strategies. One such approach was introduced by Friedman and Rafsky [1979], who employed the minimal spanning tree (MST) as

*Corresponding author: markatou@buffalo.edu

†gsaracen@buffalo.edu

a multivariate ordered list. The authors extended the univariate run-based test introduced by Wald and Wolfowitz [1940] and the univariate two-sample Kolmogorov-Smirnov test. Furthermore, the authors also proposed a modified version of the Kolmogorov-Smirnov test to address its relatively low power against scale alternatives. Similarly, Biswas et al. [2014] adopted the shortest Hamiltonian path instead of MST as ranking strategy for multivariate observations, Chen and Friedman [2017] presented a test statistic based on a similarity graph. Another approach, proposed by Bickel [1969] utilized Fisher’s permutation principle to construct a multivariate two-sample Smirnov test, and Cao and Van Keilegom [2006] introduced a local empirical likelihood test with a semi-parametric extension for the multivariate two-sample GoF problem. In addition to graph-based and permutation-based methods, general distance measures have been widely adopted to deal with multivariate two-sample GoF testing, where the distance does not necessarily satisfy all the properties in the mathematical definition. Examples of such distance-based tests include Henze [1988], Schilling [1986], Mondal et al. [2015], Barakat et al. [1996], Chen et al. [2013], Hall and Tajvidi [2002], Baringhaus and Franz [2004], Székely et al. [2004], Biswas and Ghosh [2014], Liu and Modarres [2011], Anderson et al. [1994], Fernández et al. [2008]. Among these, Rosenbaum [2005] introduced a two-sample test based on crossmatch of inter-point distances. The use of distances in addressing the multivariate two-sample goodness-of-fit problem has attracted attention not only from the field of statistics but also from various other disciplines. For example, Aslan and Zech [2005], from the field of physics, constructed a multivariate GoF test using a positive definite distance function to assess how accurately a model fits the observed data. In biology, Szabo et al. [2002] considered a negative quadratic distance to identify a subset of genes that differ the most. In the machine learning community, Gretton et al. [2012] proposed a test called Maximum Mean Discrepancy (MMD) which relies on the properties of the kernel mean embedding theory and it can be used with large samples and high dimensional datasets. Furthermore, Mitchell et al. [2022] described how certain measures of statistical distance can be implemented as diagnostics for simulations involving charged-particle beams. We note, the operating characteristics of several of the tests mentioned above were studied in Chen and Markatou [2020].

The multivariate k -sample goodness-of-fit problem extends the two-sample case to the scenario where there are more than two groups or samples to compare. In this setting it is of interest to determine whether the distributions of k groups differ significantly from each other. To address this problem, various statistical techniques have been developed. For example, Kiefer [1959], Wolf and Naus [1973] and Scholz and Stephens [1987] extended the traditional Kolmogorov-Smirnov, Cramér-von Mises and Anderson-Darling tests, introduced for the case of two distributions, for treating the k -sample problem. Zhang and Wu [2007] proposed a procedure based on likelihood ratio obtaining more powerful tests than the aforementioned approaches. Husková and Meintanis [2008] introduced multivariate tests based on the weighted L_2 distance between empirical characteristic functions; Hlávka et al. [2021] adopted the same approach for constructing tests of serial independence for functional data, and Rizzo and Székely [2016] proposed a multivariate k -sample test statistic based on Energy-statistics.

Kernel-based methods have gained popularity also for the k -sample problem due to their ability to handle high-dimensional data. We note that Balogoun et al. [2018] extended the kernel-based approach of Harchaoui et al. [2008], which utilizes the maximum Fisher discriminant ratio, to the multivariate k -sample problem. Furthermore, Balogoun et al. [2022] proposed a k -sample test for functional data by introducing a generalization

of the MMD.

In this article, our interest centers in developing novel GoF tests inspired by the kernel-based quadratic distances (KBQDs) introduced by Lindsay et al. [2008]. Quadratic distances are of interest for a variety of reasons including the following: (i) several important statistics such as Pearson’s Chi-squared and Cramér-von Mises are exactly quadratic and many other distances are asymptotically quadratic - a valid von Mises expansion establishes their distributional equivalence to a quadratic distance; (ii) the empirical quadratic distance between two distributions has a relatively simple asymptotic theory; (iii) a simple interpretation of the distance as risk is possible; (iv) if minimum distance estimation is used, a simple analysis of the information potentially lost at the model is possible; (v) simple connection and interpretation in terms of robustness can be made (see Markatou et al. [2017]). The kernel-based quadratic distance has been used to construct the multivariate one-sample goodness-of-fit tests by Lindsay et al. [2014], and the asymptotic distribution under the composite null hypothesis and alternative hypothesis were also studied.

Our contributions are as follows. We introduce a unified framework for the study of two-sample and k -sample tests that is based on the novel concept of *matrix distance*. The elements of this matrix distance are used to derive two omnibus test statistics for testing equality of distributions of k samples, and the two-sample statistic is derived as a special case of the k -sample statistic. We derive the asymptotic properties of the matrix distance and of the two test statistics under the null hypothesis when the kernel matrix has the form $\mathbf{K}(\mathbf{x}, \mathbf{y}) = (k^{\frac{1}{2}}(\mathbf{x}, \mathbf{y})\mathbf{1})(k^{\frac{1}{2}}(\mathbf{x}, \mathbf{y})\mathbf{1})^\top$, and address practical aspects related to the implementation of the test statistics. We further evaluate the performance of the k -sample and two-sample tests through a comprehensive simulation study. We demonstrate that the proposed tests exhibit high power against asymmetric alternatives that are close to the null hypothesis and with small sample size, as well as in the $k \geq 3$ sample comparison, for dimension $d > 2$ and all sample sizes. To ensure ease of use, the proposed test statistics are readily available in the package `QuadratiK`, implemented both in R and Python. By presenting a unified framework within which the k - and two-sample testing can be discussed and a comprehensive analysis of relevant testing procedures, we aim to contribute powerful tools and practical guidance for assessing the fit of distributions.

The rest of the paper is organized as follows. Section 2 provides the main concepts related to the kernel-based quadratic distances. In Section 3 we introduce the kernel-based matrix distance along with the derived k -sample test statistics, and we investigate the asymptotic properties of the matrix distance and of the test statistics. Considerations regarding the implementation of the proposed test statistics are presented in Section 4. We evaluate the performance of the two-sample and k -sample tests through simulation studies and a real data application in Section 5. Finally, concluding remarks are provided in Section 6. Relevant proofs and additional simulation results can be found in the Supplementary Material.

2 Kernel-based quadratic distances

Consider two probability measures F and G , and a non-negative definite symmetric kernel function K , possibly depending on G . The Kernel-Based Quadratic Distance (KBQD)

between F and G is defined as

$$d_K(F, G) = \iint K(\mathbf{s}, \mathbf{t}) d(F - G)(\mathbf{s}) d(F - G)(\mathbf{t}). \quad (1)$$

KBQD tests, as indicated by the name, depend on kernels. An interesting family of kernel functions is the family of *diffusion kernels* [Ding et al., 2023]. Examples of diffusion kernels include the normal kernel and the Poisson kernel. These kernels are probability kernels and satisfy the diffusion equation given by

$$K_{t_1+t_2}(\mathbf{x}, \mathbf{y}) = \int K_{t_1}(\mathbf{x}, \mathbf{s}) K_{t_2}(\mathbf{s}, \mathbf{y}) d\mathbf{s},$$

where t_1 and t_2 are the associated kernel parameters. Lindsay et al. [2008] pointed out that the kernel function generating a particular distance was not unique and introduced the model centered kernel. The G -centered kernel, K_G , of the kernel K is defined as

$$K_G(\mathbf{s}, \mathbf{t}) = K(\mathbf{s}, \mathbf{t}) - K(\mathbf{s}, G) - K(G, \mathbf{t}) + K(G, G), \quad (2)$$

where

$$\begin{aligned} K(\mathbf{s}, G) &= \int K(\mathbf{s}, \mathbf{t}) dG(\mathbf{t}), & K(G, \mathbf{t}) &= \int K(\mathbf{s}, \mathbf{t}) dG(\mathbf{s}), \\ \text{and } K(G, G) &= \iint K(\mathbf{s}, \mathbf{t}) dG(\mathbf{s}) dG(\mathbf{t}). \end{aligned}$$

The kernel K_G generates the same KBQD as the kernel K , and plays a crucial role in deriving the asymptotic distribution of the kernel-based multivariate GoF test statistics proposed in this article. The centered kernel-based quadratic distance has been used to construct the multivariate one-sample GoF tests by Lindsay et al. [2014]. In this context, let G be a known null distribution. We wish to assess whether the distribution F follows G , i.e. $H_0 : F = G$. Centering the kernel with respect to G , the corresponding KBQD can be written as $d(F, G) = \iint K_G(\mathbf{s}, \mathbf{t}) dF(\mathbf{s}) dF(\mathbf{t})$.

3 Kernel-based matrix distance and k-sample test

In this section, we introduce the concept of a matrix distance that provides a unification of the k -sample problem, where $k \geq 3$, with the two-sample problem. Consider the k -sample GoF problem where interest centers in testing the null hypothesis $H_0 : F_1 = \dots = F_k$, against the alternative $H_1 : F_i \neq F_j$, for some $1 \leq i \neq j \leq k$. Consider random samples of i.i.d. observations $\mathbf{x}_1^{(i)}, \mathbf{x}_2^{(i)}, \dots, \mathbf{x}_{n_i}^{(i)} \sim F_i$ and let \hat{F}_i be the corresponding empirical distribution function. Assume that under the null hypothesis all the compared distributions are equal to some unknown distribution \bar{F} , that is, $F_1 = \dots = F_k = \bar{F}$. Let $K(\cdot, \cdot)$ be a non-negative definite kernel function. We define the $k \times k$ matrix distance $\mathbf{D} = (D_{ij})$ with respect to kernel K , as the matrix with ij -th element given by

$$D_{ij} = \iint K(\mathbf{x}, \mathbf{y}) d(F_i - \bar{F})(\mathbf{x}) d(F_j - \bar{F})(\mathbf{y}), \quad i, j \in \{1, \dots, k\}.$$

By centering the kernel function with respect to the distribution \bar{F} , we have

$$D_{ij} = \iint K_{\bar{F}}(\mathbf{x}, \mathbf{y}) dF_i(\mathbf{x}) dF_j(\mathbf{y}). \quad (3)$$

Employing the empirical distribution functions \hat{F}_i , $i \in \{1, \dots, k\}$, the empirical version of the matrix distance \hat{D}_n has as off-diagonal elements the V -statistics

$$\hat{D}_{ij} = \frac{1}{n_i n_j} \sum_{\ell=1}^{n_i} \sum_{r=1}^{n_j} K_{\bar{F}}(\mathbf{x}_\ell^{(i)}, \mathbf{x}_r^{(j)}), \quad \text{for } i \neq j$$

and in the diagonal the U -statistics

$$\hat{D}_{ii} = \frac{1}{n_i(n_i - 1)} \sum_{\ell=1}^{n_i} \sum_{r \neq \ell}^{n_i} K_{\bar{F}}(\mathbf{x}_\ell^{(i)}, \mathbf{x}_r^{(i)}), \quad \text{for } i = j.$$

Computational considerations are important for kernel selection. For example, if a d -dimensional multivariate normal distribution is assumed under the null hypothesis, we would use the multivariate normal kernel and center it with a multivariate normal distribution with mean and variance matrix estimated from the sample. However, in practice the tested distributions F_i , $i \in \{1, \dots, k\}$, are usually unknown, as well as the true common distribution \bar{F} . Then, we propose a non-parametric centering using the weighted average distribution

$$\bar{F} = \frac{n_1 \hat{F}_1 + \dots + n_k \hat{F}_k}{n}, \quad \text{with } n = \sum_{i=1}^k n_i.$$

The concept of matrix distance can be generalized as follows. Consider an arbitrary vector of kernels $\mathbf{k}^\top(\mathbf{x}, \mathbf{t}) = (k_1(\mathbf{x}, \mathbf{t}), \dots, k_d(\mathbf{x}, \mathbf{t}))$. The construction

$$\mathbf{K}(\mathbf{x}, \mathbf{y}) = \int \mathbf{k}(\mathbf{x}, \mathbf{t}) \mathbf{k}^\top(\mathbf{y}, \mathbf{t}) d\mathbf{u}(\mathbf{t}) \quad (4)$$

creates a matrix kernel so that the corresponding matrix distance between F and G satisfies the usual definition of a quadratic distance. Before we define formally the concept of a matrix distance, we note here that the matrix kernel defined in equation (4) is generally not symmetric. This matrix kernel can be symmetrized if we define

$$\mathbf{K}(\mathbf{x}, \mathbf{y}) = \frac{1}{2} \int (\mathbf{k}^\top(\mathbf{x}, \mathbf{t}) \mathbf{k}(\mathbf{y}, \mathbf{t}) + \mathbf{k}^\top(\mathbf{y}, \mathbf{t}) \mathbf{k}(\mathbf{x}, \mathbf{t})) d\mathbf{u}(\mathbf{t}).$$

If the elements of the vector of kernels $\mathbf{k}^\top(\mathbf{x}, \mathbf{t})$ are nonnegative definite kernels, then $\mathbf{K}(\mathbf{x}, \mathbf{y})$ is a nonnegative definite kernel matrix. Indeed, considering the matrix kernel in equation (4), for every $\mathbf{a} \in \mathbb{R}^d$

$$\begin{aligned} \mathbf{a}^\top \mathbf{K}(\mathbf{x}, \mathbf{y}) \mathbf{a} &= \mathbf{a}^\top \left(\int \mathbf{k}(\mathbf{x}, \mathbf{t}) \mathbf{k}^\top(\mathbf{y}, \mathbf{t}) d\mathbf{u}(\mathbf{t}) \right) \mathbf{a} \\ &= \sum_{i=1}^d \sum_{j=1}^d a_i \left(\int k_i(\mathbf{x}, \mathbf{t}) k_j^\top(\mathbf{y}, \mathbf{t}) d\mathbf{u}(\mathbf{t}) \right) a_j \geq 0, \end{aligned}$$

given that the product of nonnegative definite kernels is nonnegative definite. As a special case, if the elements of the kernel vector $\mathbf{k}(\mathbf{x}, \mathbf{t})$ are root kernels [Lindsay et al., 2014], then the kernel $\mathbf{K}(\mathbf{x}, \mathbf{y})$ generates a quadratic matrix distance with elements equal to D_{ij} defined above.

Definition 1. Let F, G be two probability distributions and $\mathbf{K}(\mathbf{x}, \mathbf{y})$ a matrix kernel defined by (4). Then, the matrix distance between F, G is defined as

$$d_K(F, G) = \iint \mathbf{K}(\mathbf{x}, \mathbf{y}) d(F - G)(\mathbf{x}) d(F - G)(\mathbf{y})$$

with $d_K(F, G) \geq 0$ in a matrix sense.

The matrix distance $d_K(F, G)$ defined above is therefore a nonnegative matrix, and each of its elements is greater than or equal to 0, i.e. $(d_K(F, G))_{ij} \geq 0, \forall i, j \in \{1, \dots, d\}$. Note that, even if the kernel matrix $\mathbf{K}(\mathbf{x}, \mathbf{y})$ defined in (4) is not symmetric, the distance matrix $d_K(F, G)$ is symmetric. This is because of the following proposition.

Proposition 1. *Let F, G be two probability distributions and $\mathbf{K}(\mathbf{x}, \mathbf{y})$ the kernel matrix given in (4), with $\mathbf{k}^\top(\mathbf{x}, \mathbf{t})$ being a vector of nonnegative definite kernels. Then, the matrix distance $d_K(F, G)$ is symmetric.*

Note that, we do not require $\mathbf{k}(\mathbf{x}, \mathbf{t})$ to be a vector of symmetric kernels for $d_K(F, G)$ to be symmetric.

Finally, we present the following example which illustrates the construction of the matrix distance with elements defined in equation (3) for the comparison of three samples.

Example 1 ($\mathbf{k} = \mathbf{3}$). *Consider the case $k = 3$, and the null hypothesis $H_0 : F_1 = F_2 = F_3$ against the alternative $H_1 : F_i \neq F_j$ for $i, j \in \{1, 2, 3\}$. Let $\mathbf{x}_1^{(i)}, \dots, \mathbf{x}_{n_1}^{(i)} \sim F_i$ be a i.i.d. sample for $i \in \{1, 2, 3\}$ and $\bar{F} = (n_1 F_1 + n_2 F_2 + n_3 F_3)/n$ with $n = n_1 + n_2 + n_3$. Then, the introduced matrix distance has the form*

$$\mathbf{D} = \begin{pmatrix} D_{11} & D_{12} & D_{13} \\ D_{21} & D_{22} & D_{23} \\ D_{31} & D_{32} & D_{33} \end{pmatrix},$$

that is

$$\begin{pmatrix} \iint K_{\bar{F}}(\mathbf{x}, \mathbf{y}) dF_1(\mathbf{x}) dF_1(\mathbf{y}) & \iint K_{\bar{F}}(\mathbf{x}, \mathbf{y}) dF_1(\mathbf{x}) dF_2(\mathbf{y}) & \iint K_{\bar{F}}(\mathbf{x}, \mathbf{y}) dF_1(\mathbf{x}) dF_3(\mathbf{y}) \\ \iint K_{\bar{F}}(\mathbf{x}, \mathbf{y}) dF_2(\mathbf{x}) dF_1(\mathbf{y}) & \iint K_{\bar{F}}(\mathbf{x}, \mathbf{y}) dF_2(\mathbf{x}) dF_2(\mathbf{y}) & \iint K_{\bar{F}}(\mathbf{x}, \mathbf{y}) dF_2(\mathbf{x}) dF_3(\mathbf{y}) \\ \iint K_{\bar{F}}(\mathbf{x}, \mathbf{y}) dF_3(\mathbf{x}) dF_1(\mathbf{y}) & \iint K_{\bar{F}}(\mathbf{x}, \mathbf{y}) dF_3(\mathbf{x}) dF_2(\mathbf{y}) & \iint K_{\bar{F}}(\mathbf{x}, \mathbf{y}) dF_3(\mathbf{x}) dF_3(\mathbf{y}) \end{pmatrix},$$

where $K_{\bar{F}}$ denotes the kernel centered with respect to \bar{F} . Notice that, the elements in the diagonal correspond to the kernel-based quadratic distances between each F_i and \bar{F} , while the off diagonal elements measure the contrasts for each pair of the tested distributions. The kernel function is centered with respect to the weighted average distribution $\bar{F} = (n_1 F_1 + n_2 F_2 + n_3 F_3)/(n_1 + n_2 + n_3)$ and the matrix distance \mathbf{D} is orthogonal to the vector $(n_1/n, n_2/n, n_3/n)^\top$. Alternatively, an equally weighted \bar{F} could be used, which would then create a matrix orthogonal to $(1, 1, 1)^\top$. In this case, the eigenvectors are contrasts, aiding the interpretation of results.

An eigenanalysis of the matrix distance provides the following information. The leading eigenvalue of \mathbf{D} gives the linear combination $a_1(F_1 - \bar{F}) + a_2(F_2 - \bar{F}) + a_3(F_3 - \bar{F})$ that is most different from zero. The null space of the matrix \mathbf{D} consists of linear combinations $\sum_{i=1}^3 b_i(F_i - \bar{F}) = 0$. For example, if $F_3 - \bar{F} = 0$, which occurs when $F_3 = n_1(n_1 + n_2)^{-1}F_1 + n_2(n_1 + n_2)^{-1}F_2$, then the vector $(1, -1, 0)$ is in the null space of \mathbf{D} .

We now investigate the asymptotic distribution of the matrix distance $\hat{\mathbf{D}}_n$ under the null hypothesis. Notice that, each element of this matrix distance depends on the same symmetric root kernel $k^{\frac{1}{2}}(\mathbf{x}, \mathbf{t})$, hence the ij -element of the matrix distance $\mathbf{K}(\mathbf{x}, \mathbf{y})$ is given as $\int k^{\frac{1}{2}}(\mathbf{x}, \mathbf{t})k^{\frac{1}{2}}(\mathbf{t}, \mathbf{y})du(\mathbf{t})$. See Lindsay et al. [2014] for a discussion on the role of root kernels in this context. The first result is given by the spectral decomposition of the centered kernel under \bar{F} .

Proposition 2. Let \mathbf{D} be the matrix distance with elements defined in equation (3). The matrix distance \mathbf{D} can be written as

$$\mathbf{D} = \sum_{p=1}^{\infty} \lambda_p \tilde{\phi}_p \tilde{\phi}_p^\top,$$

where $\tilde{\phi}_p = (\bar{\phi}_{p,1}, \dots, \bar{\phi}_{p,k})$ is the k -dimensional vector with entries, given as

$$\bar{\phi}_{p,i} = \int \phi_p(\mathbf{x}) dF_i(\mathbf{x}),$$

are averages of mean-zero, variance-1 random variables uncorrelated with respect to p .

Consider random samples of i.i.d. observations $\mathbf{x}_1^{(i)}, \mathbf{x}_2^{(i)}, \dots, \mathbf{x}_{n_i}^{(i)} \sim F_i$, $i \in \{1, \dots, k\}$. The asymptotic distribution of the matrix distance $\hat{\mathbf{D}}_n$ under the null hypothesis is provided as follows.

Proposition 3. Let $K_{\bar{F}}$ be the kernel centered by the common distribution \bar{F} such that

- (i) $\int K_{\bar{F}}(\mathbf{t}, \mathbf{t}) d\bar{F}(\mathbf{t}) < \infty$;
- (ii) $\iint K_{\bar{F}}^2(\mathbf{s}, \mathbf{t}) d\bar{F}(\mathbf{s}) d\bar{F}(\mathbf{t}) < \infty$;

Then, under the null hypothesis $H_0 : F_1 = \dots = F_k$ we have that

$$n\hat{\mathbf{D}}_n \xrightarrow{d} W^* = \sum_{p=1}^{\infty} \lambda_p W_{k,p}, \quad (5)$$

where λ_p are the nonzero eigenvalues of $K_{\bar{F}}$; $W_{k,p}$, $p = 1, 2, \dots$, are independent random variables that follow the k -dimensional Wishart distribution with covariance matrix \mathbf{V} and 1 degree of freedom, denoted as $W_{k,p} \sim \mathcal{W}_k(1, \mathbf{V})$, and \mathbf{V} is a diagonal matrix with $V_{ii} = 1/\rho_i$ with $\rho_i = \lim_{n, n_i \rightarrow \infty} n_i/n$ and $0 < \rho_i < 1$.

Example 2 (k=3 – Continued). For $k = 3$, when the kernel is centered with respect to the weighted average distribution \bar{F} the covariance matrix of the independent Wishart distribution is given as $\mathbf{V} = \text{diag}(n/n_1, n/n_2, n/n_3)$.

Notice that, if the non-centered kernel is employed the spectral decomposition of the matrix distance \mathbf{D} is given as

$$\mathbf{D} = \sum_{p=1}^{\infty} \lambda_p \phi_p^* (\phi_p^*)^\top$$

with $\phi_p^* = (\bar{\phi}_{p,1} - \bar{\phi}_p, \dots, \bar{\phi}_{p,k} - \bar{\phi}_p)$, where

$$\bar{\phi}_p = \int \phi_p(\mathbf{x}) d\bar{F}(\mathbf{x}).$$

Let $\boldsymbol{\pi}^\top = (n_1/n, \dots, n_k/n)$ and let $\mathbf{1}$ denote a vector of ones. then, ϕ_p^* can be written as $\phi_p^* = \mathbf{I}^* \tilde{\phi}_p$ with $\mathbf{I}^* = \mathbf{I} - \mathbf{1}\boldsymbol{\pi}^\top$, and in this case the variance of the Wishart distribution is given as $\mathbf{V}^* = \mathbf{I}^* \mathbf{A} (\mathbf{I}^*)^\top$. For $k = 3$

$$\mathbf{V}^* = \begin{pmatrix} \frac{n_{(1)}^2}{n_1 n^2} & \frac{n_{(1)}}{n^2} & \frac{n_{(1)}}{n^2} \\ \frac{n_{(2)}}{n^2} & \frac{n_{(2)}^2}{n_2 n^2} & \frac{n_{(2)}}{n^2} \\ \frac{n_{(3)}}{n^2} & \frac{n_{(3)}}{n^2} & \frac{n_{(3)}^2}{n_3 n^2} \end{pmatrix},$$

where $n_{(i)}$ denotes the sum of the samples sizes except for n_i . Note that, the matrix \mathbf{V}^* is not full rank.

3.1 k -sample omnibus tests

In order to perform hypothesis testing in the k -sample problem against general alternatives $H_1 : F_i \neq F_j$, for some $1 \leq i \neq j \leq k$, we propose two omnibus tests derived from the matrix distance. Specifically, we consider the trace statistic

$$\text{trace}(\hat{\mathbf{D}}_n) = \sum_{i=1}^k \hat{D}_{ii}. \quad (6)$$

and T_n , derived considering all the possible pairwise comparisons in the k -sample null hypothesis, given as

$$T_n = (k-1)\text{trace}(\hat{\mathbf{D}}_n) - 2 \sum_{i=1}^k \sum_{j>i}^k \hat{D}_{ij}. \quad (7)$$

The asymptotic distribution of T_n under the null hypothesis is provided in the following proposition, while the asymptotic distribution of $\text{trace}(\hat{\mathbf{D}}_n)$ is derived as a special case.

Proposition 4. *Let $n = n_1 + \dots + n_k$ and let $K_{\bar{F}}$ be the kernel centered by the common distribution \bar{F} such that*

- (i) $\int K_{\bar{F}}(\mathbf{t}, \mathbf{t}) d\bar{F}(\mathbf{t}) < \infty$;
- (ii) $\iint K_{\bar{F}}^2(\mathbf{s}, \mathbf{t}) d\bar{F}(\mathbf{s}) d\bar{F}(\mathbf{t}) < \infty$;
- (iii) $K_{\bar{F}}$ is continuous at (\mathbf{s}, \mathbf{s}) for almost all \mathbf{s} with respect to the measure \bar{F} .

Then, under the null hypothesis $H_0 : F_1 = \dots = F_k = \bar{F}$ we have that

$$nT_n \xrightarrow{d} \chi^* = \sum_{p=1}^{\infty} \lambda_p \left[\sum_{i=1}^k \sum_{j>i}^k \left(\frac{1}{\sqrt{\rho_i}} Z_{ip} - \frac{1}{\sqrt{\rho_j}} Z_{jp} \right)^2 - \sum_{i=1}^k \frac{1}{\rho_i} \right] \text{ as } n_i, n \rightarrow \infty, \quad (8)$$

where Z_{1p}, \dots, Z_{kp} are k independent random variables that follow the standard normal distribution; λ_p are the nonzero eigenvalues of $K_{\bar{F}}$; $\rho_i = \lim_{n_i, n \rightarrow \infty} n_i/n$, $i \in \{1, \dots, k\}$ and $0 < \rho_i < 1$.

Corollary 1. *Consider the same assumptions of proposition 4. Then, under the null hypothesis $H_0 : F_1 = \dots = F_k = \bar{F}$ we have that*

$$n\text{trace}(\hat{\mathbf{D}}_n) \xrightarrow{d} \sum_{p=1}^{\infty} \lambda_p \sum_{i=1}^k \frac{1}{\rho_i} (Z_{ip}^2 - 1) \text{ as } n_i, n \rightarrow \infty, \quad (9)$$

where Z_{1p}, \dots, Z_{kp} are k independent random variables that follow the standard normal distribution; λ_p are the nonzero eigenvalues of $K_{\bar{F}}$; $\rho_i = \lim_{n_i, n \rightarrow \infty} n_i/n$, $i \in \{1, \dots, k\}$ and $0 < \rho_i < 1$.

3.2 Two-sample Goodness-of-Fit Tests

As highlighted in the Introduction, the problem of testing the general non parametric hypothesis $H_0 : F = G$ versus the alternative $H_1 : F \neq G$ with F and G unknown, is of particular interest. Assume that $\mathbf{x}_1, \dots, \mathbf{x}_n$ is a random sample from the distribution of the random variable $\mathbf{X} \sim F$ and $\mathbf{y}_1, \dots, \mathbf{y}_m$ is a random sample from the distribution of

the random variable $\mathbf{Y} \sim G$. The KBQD test statistics in equations (7) and (6) reduce to

$$\text{trace}(\hat{\mathbf{D}}_n) = \frac{1}{n(n-1)} \sum_{i=1}^n \sum_{j \neq i}^n K_{\bar{F}}(\mathbf{x}_i, \mathbf{x}_j) + \frac{1}{m(m-1)} \sum_{i=1}^m \sum_{j \neq i}^m K_{\bar{F}}(\mathbf{y}_i, \mathbf{y}_j),$$

and

$$\begin{aligned} T_{n,m} = & \frac{1}{n(n-1)} \sum_{i=1}^n \sum_{j \neq i}^n K_{\bar{F}}(\mathbf{x}_i, \mathbf{x}_j) - \frac{2}{nm} \sum_{i=1}^n \sum_{j=1}^m K_{\bar{F}}(\mathbf{x}_i, \mathbf{y}_j) \\ & + \frac{1}{m(m-1)} \sum_{i=1}^m \sum_{j \neq i}^m K_{\bar{F}}(\mathbf{y}_i, \mathbf{y}_j). \end{aligned} \quad (10)$$

Notice that, the kernel function is centered with respect to

$$\bar{F} = \frac{n}{n+m} \hat{F} + \frac{m}{n+m} \hat{G},$$

and the two-sample test statistic is not modified by the centering distribution, as shown in the following Lemma.

Lemma 1. *For any centering distribution F^**

$$d_K(F, G) = d_{K_{F^*}}(F, G).$$

The asymptotic distribution of the two-sample KBQD test statistics under the null hypothesis is given by the result stated in Proposition 4 and Corollary 1. The case $k = 2$ is considered in section S1 of the Supplementary Material. Details with respect to the derivation of the asymptotic results for the statistic $D_{n,m}$ in the two-sample problem can be found in Chen [2018].

3.3 Kernel-based tests in the literature

At this point, it is instructive to visit constructions of kernel tests that exist in the literature. Rao [1982] introduced the concept of an exact quadratic distance for discrete population distributions named *quadratic entropy*. Rao's definition of quadratic entropy is as follows:

$$Q(P) = \iint K(\mathbf{x}, \mathbf{y}) dP(\mathbf{x}) dP(\mathbf{y}),$$

where $K(\mathbf{x}, \mathbf{y})$ is a measurable, conditionally negative definite kernel, i.e. the kernel satisfies the condition

$$\sum_{i=1}^n \sum_{j=1}^n K(\mathbf{x}_i, \mathbf{x}_j) a_i a_j \leq 0,$$

for all $\mathbf{x}_1, \dots, \mathbf{x}_n$ that belong to the sample space and any choice of real numbers a_1, \dots, a_n such that $\sum_{i=1}^n a_i = 0$. Quadratic entropy has several interesting properties, such as convexity of Jensen differences of all orders (see Rao [1982]). This is the concept closest to the work presented here. Other relevant works are as follows.

Let \mathbf{X} and \mathbf{Y} be random variables on the sample space \mathcal{X} with corresponding probability measures F and G . Given \mathcal{F} , a class of functions $f : \mathcal{X} \rightarrow \mathbb{R}$, the maximum mean discrepancy is defined as

$$\text{MMD}[\mathcal{F}, F, G] := \sup_{f \in \mathcal{F}} (E_{\mathbf{X}}[f(\mathbf{X})] - E_{\mathbf{Y}}[f(\mathbf{Y})]).$$

Gretton et al. [2012] considers as \mathcal{F} the unit ball in a reproducing kernel Hilbert space (RKHS) \mathcal{H} , which has an associated kernel function K . The kernel mean embedding of the random variables \mathbf{X} and \mathbf{Y} are given as $\mu_{\mathbf{X}} = E_{\mathbf{X}}[K(\mathbf{X}, \cdot)]$ and $\mu_{\mathbf{Y}} = E_{\mathbf{Y}}[K(\cdot, \mathbf{Y})]$. Within this setting the **squared** MMD has the form

$$\text{MMD}^2(F, G) := \|\mu_{\mathbf{X}} - \mu_{\mathbf{Y}}\|_{\mathcal{H}}^2,$$

where $\|\cdot\|_{\mathcal{H}}$ denotes the Hilbert space norm. Then, the corresponding U -statistic is given by

$$\begin{aligned} \text{MMD}^2(\mathbf{X}, \mathbf{Y}) &= \frac{1}{n(n-1)} \sum_{i=1}^n \sum_{j \neq i}^n K(x_i, x_j) - \frac{2}{nm} \sum_{i=1}^n \sum_{j=1}^m K(x_i, y_j) \\ &\quad + \frac{1}{m(m-1)} \sum_{i=1}^m \sum_{j \neq i}^m K(y_i, y_j). \end{aligned}$$

The MMD formulation does not explicitly incorporate the centering of the kernel. This aspect plays a crucial role in the computation of the asymptotic distribution of the kernel-based test statistics. Furthermore, the selection of the kernel tuning parameter, as proposed by Gretton et al. [2012], is determined by the median Euclidean distance within the pooled sample. This pragmatic approach offers a direct method for parameter estimation, however, it is acknowledged that this choice does not come with a formal optimality guarantee.

Another powerful method for comparing statistical distributions is given by the energy distance, defined as

$$\mathcal{E}(X, Y) = 2E[\|X - Y\|] - E[\|X - X'\|] - E[\|Y - Y'\|],$$

where X' and Y' are independent and identically distributed copies of X and Y , respectively. The energy distance is a measure of the statistical distance between the distributions of the random vectors \mathbf{X} and \mathbf{Y} . The corresponding U -statistic for the energy distance is

$$\mathcal{E}_{n,m}(X, Y) = \frac{2}{nm} \sum_{i=1}^n \sum_{j=1}^m \|x_i - y_j\| - \frac{1}{n^2} \sum_{i=1}^n \sum_{j=1}^n \|x_i - x_j\| - \frac{1}{m^2} \sum_{i=1}^m \sum_{j=1}^m \|y_i - y_j\|.$$

The presented literature belongs to the class of methods known as integral probability metrics, which measure the distance between probability distributions based on expectations of functions belonging to a certain class. Considering the MMD and energy distances the primary difference between these two metrics lies in the function space \mathcal{F} : MMD utilizes functions from an RKHS defined by a kernel, whereas energy distance uses Euclidean distance-based functions. This difference in the function space leads to different properties and performance in statistical tests. For example, energy distance has connections to the Cramér-von Mises criterion and is known for its strong performance in high-dimensional settings [Székely and Rizzo, 2013, Rizzo and Székely, 2016]. While MMD and energy distance both provide robust methods for comparing distributions, their formulations and underlying assumptions differ. MMD leverages the rich structure of RKHS, offering flexibility through kernel choice and tuning, whereas energy distance directly utilizes geometric properties of the sample space. The KBQD can encompass the presented distances through an appropriate choice of the kernel function. For example,

the energy distance can be obtained by considering the linear kernel. Lindsay et al. [2014] offered a second interpretation of the quadratic distance as the L_2 distance between the smoothed version of two probability distribution by using the root kernel, indicating the connection of the KBQD with the reproducing kernel Hilbert space formulation employed in the MMD construction.

For the k -sample problem, with null hypothesis $H_0 : F_1 = F_2 = \dots = F_k$, Balogoun et al. [2022] introduced the generalized maximum mean discrepancy (GMMD) as

$$\text{GMMD}^2(F_1, \dots, F_k, \boldsymbol{\pi}) = \sum_{i=1}^k \sum_{j \neq i}^k \pi_j \text{MMD}^2(F_i, F_j),$$

with $\boldsymbol{\pi} = (\pi_1, \dots, \pi_k) \in (0, 1)^k$ and $\sum_{i=1}^k \pi_i = 1$. Balogoun et al. [2022] considered $\pi_i = n_i/n$. Notice that the GMMD statistic coincides with the proposed T_n statistic for $\pi_i = 1$. In contrast to MMD and GMMD, the proposed KBQD test statistics takes into account the centering of the kernel, which plays a significant role in deriving the asymptotic properties of the test.

4 Numerical aspects

From a practical point of view, it is important to know how to compute the test statistic starting from the data. The first step for computing the k -sample test statistics T_n , given in equation (7), is to properly center the kernel function. In order to avoid any assumption on the common distribution \bar{F} under the null hypothesis, we consider the non-parametric centering with $\bar{F} = (n_1 F_1 + \dots + n_k F_k)/n$ where $n = \sum_{i=1}^k n_i$. Let $\mathbf{z}_1, \dots, \mathbf{z}_n$ denote the pooled sample. Following equation 2, for any $s, t \in \{\mathbf{z}_1, \dots, \mathbf{z}_n\}$, the non-parametric \bar{F} -centered kernel is given by

$$K_{\bar{F}}(\mathbf{s}, \mathbf{t}) = K(\mathbf{s}, \mathbf{t}) - \frac{1}{n} \sum_{i=1}^n K(\mathbf{s}, \mathbf{z}_i) - \frac{1}{n} \sum_{i=1}^n K(\mathbf{z}_i, \mathbf{t}) + \frac{1}{n(n-1)} \sum_{i=1}^n \sum_{j \neq i}^n K(\mathbf{z}_i, \mathbf{z}_j).$$

Chen and Markatou [2020] detailed both parametric and non-parametric centering of the test statistic for the two-sample problem. Both types of centering are implemented in the package `QuadratiK`, in R and Python [Saraceno et al., 2024], as available options when performing the two-sample test.

An aspect closely related to the implementation is the calculation of the critical value. The asymptotic distribution of the test statistic given in Proposition 4 involves the eigenvalues of the centered kernel. This step, while theoretically significant, is practically unnecessary. By employing numerical techniques such as the bootstrap, permutation and subsampling algorithms, we can compute the empirical critical value efficiently without the need for eigenvalue analysis. These methods not only simplify the process, but also ensure that the calculation is rigorous and applicable to real-world scenarios. The general algorithm for computing the critical value is illustrated in Algorithm 1.

Algorithm 1 Algorithm for the computation of the critical value.

- 1: Let B denote the number of sampling repetitions.
 - 2: Generate k -tuples, of total size n_B , from the pooled sample z_1, \dots, z_n following one of sampling method (bootstrap/permutation/subsampling);
 - 3: Compute the k -sample test statistic;
 - 4: Repeat steps 1-2 B times;
 - 5: Select the 95th quantile of the obtained list of values.
-

The main difference between the bootstrap and subsampling algorithms is that they correspond to sampling from the pooled sample with and without replacement, respectively. While in bootstrap the samples are generated with the same size, the subsampling samples have smaller sample size than the original data, i.e. $n_B = b * n$ and $b \in (0, 1]$. The determination of the "optimal" sample size n_B remains a subject without definitive guidelines. Approaches for obtaining the optimal subsamples explored in literature involve concepts of optimal subsampling probabilities. For details see Yao and Wang [2021]. We investigated the performance of Algorithm 1 with the subsampling algorithm for different choices of the subsample proportion b , through a small simulation study reported in section S2 of the Supplementary Material. In the simulation studies considered here we set $b = 0.8$. Finally, the permutation algorithm draws observations from the original data set, creating new samples that maintain the original sample size. This method aligns with the subsampling algorithm with $b = 1$, indicating that new samples are formed by sampling without replacement.

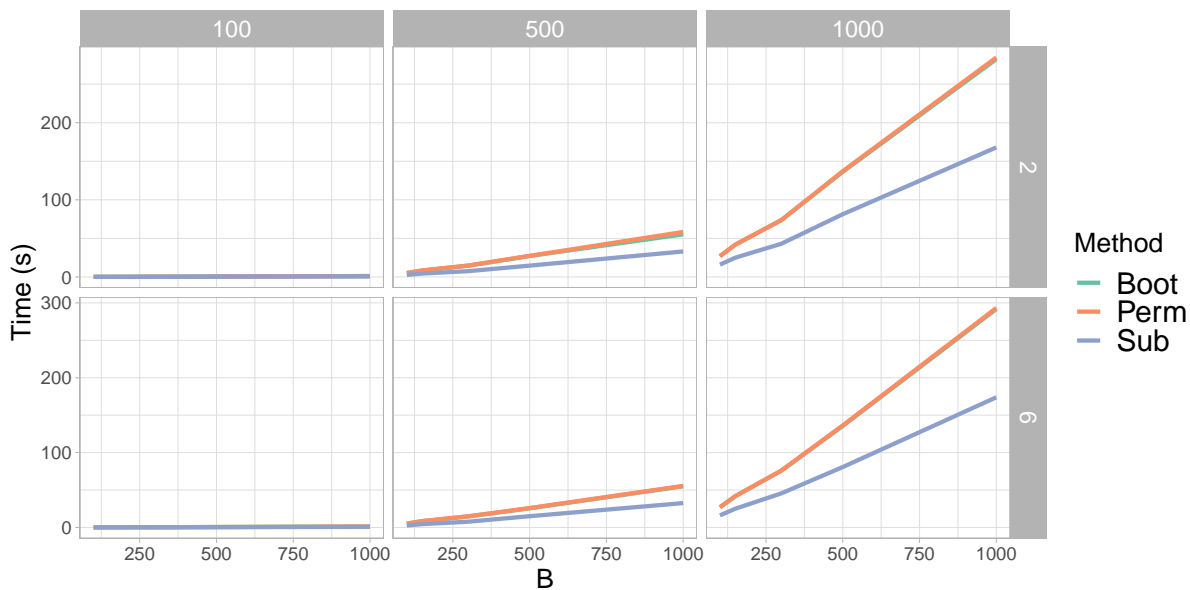


Figure 1: Computational time (seconds) for computing the KBQD test for increasing number of replications B for the bootstrap, permutation and subsampling algorithms. The sample size $n = 100, 500, 1000$ and dimension $d = 2, 6$, are indicated as headers. For the subsampling algorithm we use $b = 0.8$.

The non-parametric calculation of the critical value depends on the number of replications of the bootstrap-, permutation- or subsampling-step, denoted as B . We investigate the performance of the proposed KBQD tests with respect to different values of B , when $k = 2$. In particular, we consider $B = 100, 150, 300, 500, 1000$. We generated samples

$\mathbf{x}_1, \dots, \mathbf{x}_{n_1}$ from the normal distribution $N_d(\mathbf{0}, \mathbf{I}_d)$ and $\mathbf{y}_1, \dots, \mathbf{y}_{n_2}$ from the skew-normal distribution $SN_d(\mathbf{0}, \mathbf{I}_d, \boldsymbol{\lambda})$, where \mathbf{I}_d denotes the d -dimensional identity matrix, $\boldsymbol{\lambda} = \lambda \mathbf{1}$ and $\lambda = 0, 0.1, 0.2, 0.3$. Observations are sampled using the R package `sn`. We considered dimensions $d = 1, 2, 6$, sample size $n_1 = n_2 = 100, 500, 1000$ and $N = 1000$ replications. The tuning parameter h of the KBQD test takes values from 0.2 to 10 with a step of 0.4, denoted as $h = 0.2(0.4)10$. Figure 1 shows the mean computational time needed for computing the KBQD tests when B increases, with respect to the considered algorithms, $d = 2$ and the sample size n is indicated as header. The mean values are summarized with respect to the values of h , λ and N for a total of 100000 observations. The computational time increases linearly with increasing B . The subsampling algorithm requires about half of the time needed by bootstrap and permutation procedures. This becomes relevant for very large sample sizes. Additionally, the computational time does not increase for higher dimensions. Figure 2 shows the boxplots of critical values computed with the

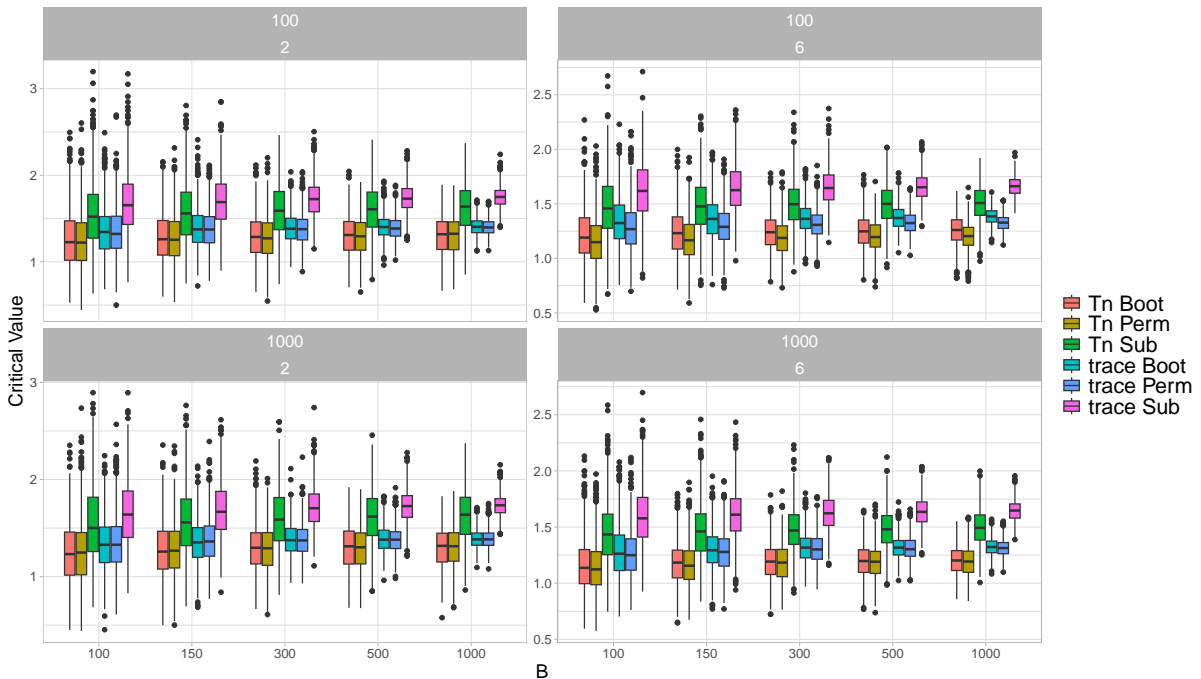


Figure 2: Boxplots of critical values of the KBQD test statistics, T_n and trace, for increasing B with respect to the bootstrap, permutation and subsampling algorithm, and different values of dimension d and sample size n , indicated as headers. $h = 2.2$ and $\lambda = 0$.

considered algorithms for $h = 2.2$ and different values of n and d , indicated as headers. The computed critical values show less variability for larger B , while there are no evident differences in terms of sample size and dimension.

Finally, we investigate if the KBQD tests are affected by the value of B , in terms of level and power. Figure 3 compares the level achieved by the KBQD tests with respect to B , for increasing h , $d = 6$ and different values of n , indicated as header. In general, subsampling achieves a lower level than the nominal level, preferring lower values of B , especially in low dimensions. For bootstrap and permutation, increasing the number of replications B improves the performance in terms of level, while for large d the differences are less evident and the achieved level is equal to the nominal one for almost all values of h . Figure 4 shows the power of the KBQD tests for the considered algorithms and

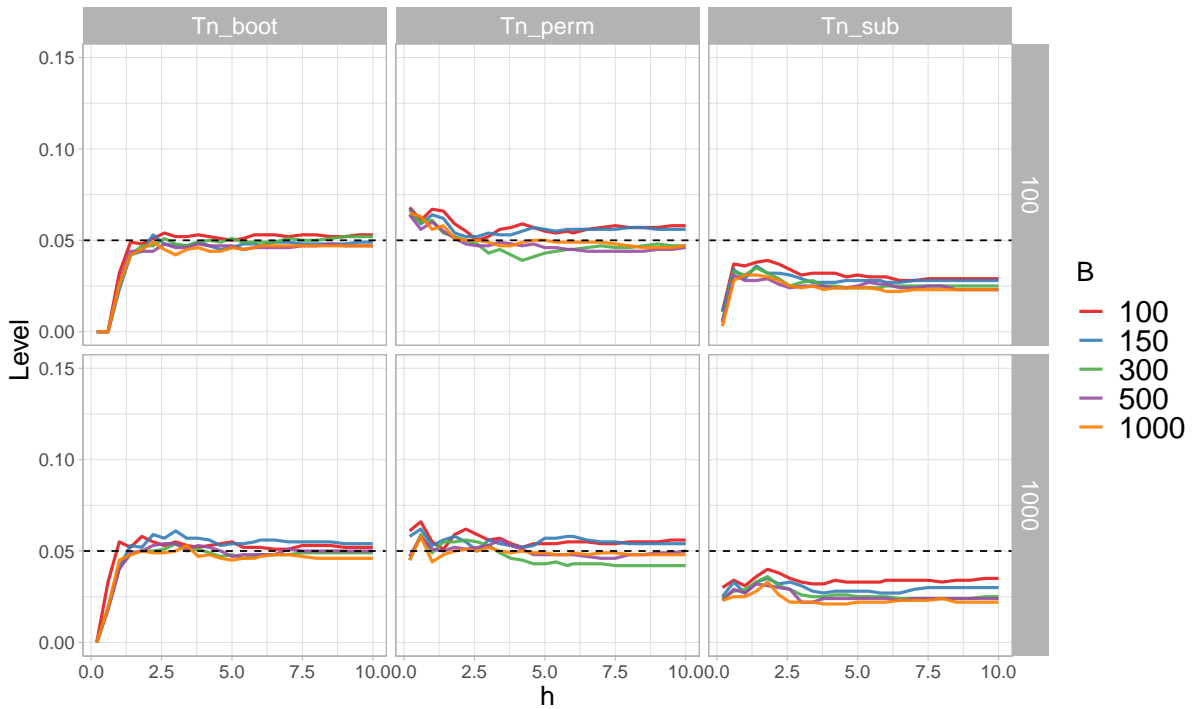


Figure 3: Level of KBQD tests for increasing h with respect to the bootstrap, permutation and subsampling algorithm, for different values of n , $N = 1000$ replications, $d = 2$. The dashed line denotes the nominal level $\alpha = 0.05$.

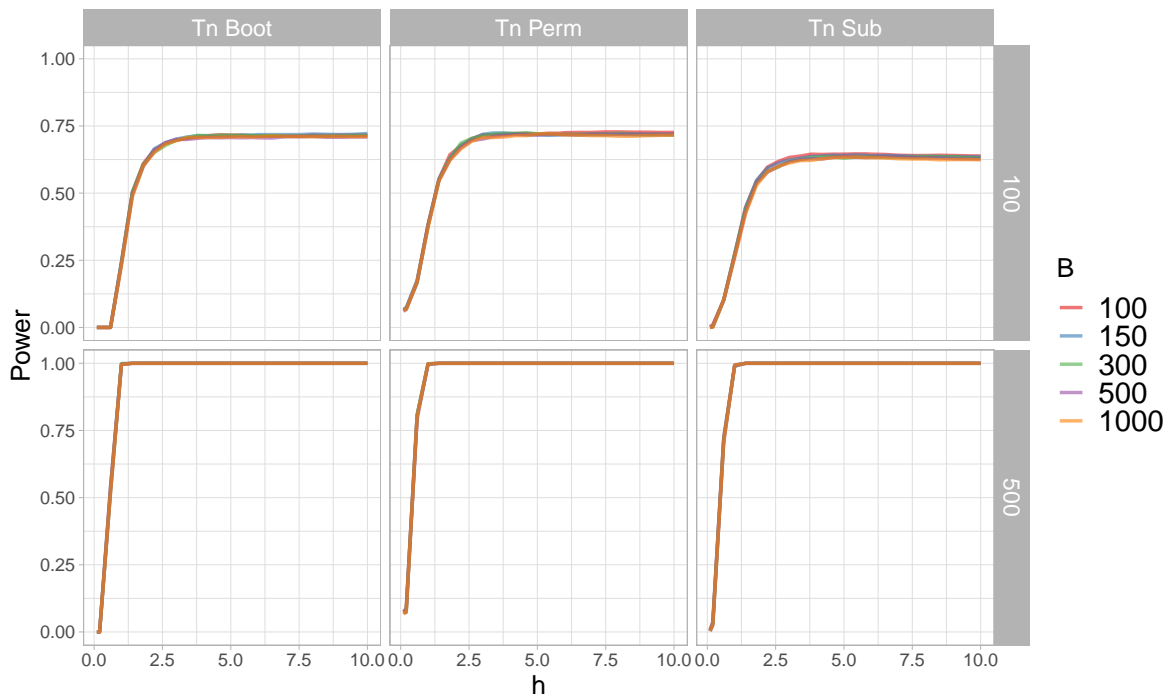


Figure 4: Power of KBQD tests for increasing h with respect to the bootstrap, permutation and subsampling algorithm, for $n = 100, 500$, $N = 1000$ replications, $d = 6$ and $\lambda = 0.3$.

the different values of B , when $n = 100, 500$, $d = 6$ and $\lambda = 0.3$. For small sample size,

the tests with lower number of replications achieve slightly higher power while for the other combinations of parameter values the obtained power does not change significantly. Complete results are reported in Section S3 of the Supplemental Material.

In summary, permutation and bootstrap sampling methods are preferred in high-dimensional spaces and small sample sizes due to their stability in performance, while subsampling is favored for large sample sizes for its lower computational time. Considering the evaluation of the performances of the KBQD tests with respect to the number of replications B reported in this section, we recommend the usage of $B = 150$ as default setting, offering a balance between statistical power, stability and computational feasibility.

Considering the performance in terms of level in Figure 3, we increased the number of replications to $N = 10000$, for dimension $d = 2, 6$ and sample size $n = 500, 1000$. The KBQD tests are computed for $B = 150$ and $h = 0.2(0.4)10$. Figure 5 presents the level of the T_n and trace statistics for each combination of dimension and sample size. The results indicate that the KBQD tests consistently maintain the nominal level regardless of the algorithm used to compute the critical value.

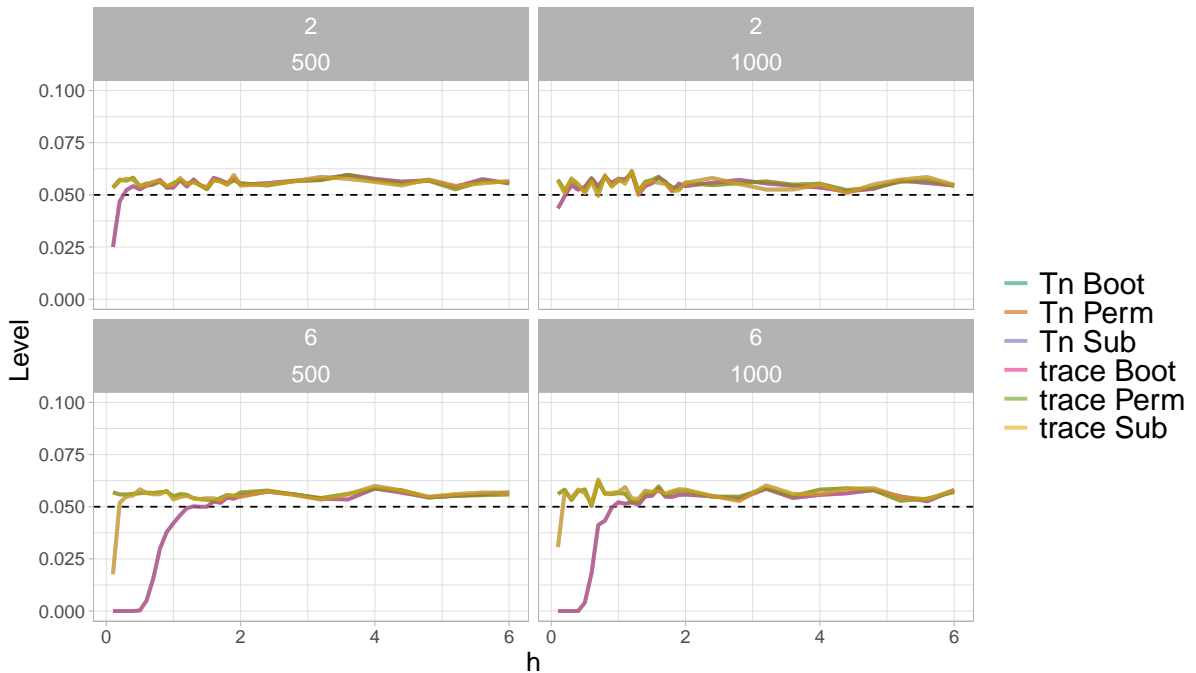


Figure 5: Level of KBQD tests for increasing h with respect to the bootstrap, permutation and subsampling algorithm, for $n = 500, 1000$, $d = 2, 6$ and $N = 10000$ replications. Samples are generated from standard normal distribution.

4.1 Selection of tuning parameter h

In the one-sample problem, Lindsay et al. [2014] proposed a strategy to select the tuning parameter of the kernel used to build the quadratic distances comparing the sensitivity of a class of kernels indexed by the tuning parameter. We properly adapt this procedure in order to select the appropriate tuning parameter for the k -sample test statistics.

Under the null hypothesis, the asymptotic distribution of the test statistics can be approximated by a normal distribution. Then, the power of the test statistics can be approximated using asymptotic normality under the alternative through the power function

$$\beta(H_1) = \mathbb{P}(T_n > z_\alpha \sigma_0) = \mathbb{P}\left(Z > \frac{z_\alpha \sigma_0 - \mathbb{E}_{H_1}(T_n)}{\sigma_1}\right),$$

where z_α is the normal critical value with level α , σ_0^2 is the variance of the test statistic T_n under the null hypothesis, and σ_1^2 is the variance of T_n under the alternative hypothesis. The procedure centers on the mid-power manifold, denoted as $\beta(H_1) = 0.5$, which simplifies the analytic computations. The selection of the tuning parameter h for the k -sample tests is outlined as follows.

- At first, select a family of target alternative hypothesis, denoted as $\{F_\delta\}$, with $\delta \geq 0$. Here, $\delta = 0$ corresponds to the null hypothesis, and increments in δ signify increasingly pronounced deviations from H_0 .
- For a given value of h , we determine the minimum δ that yields power greater than or equal to 0.5 as

$$\delta_{mid}(h) = \arg \min\{\delta : \beta_h(\delta) = 0.5\}.$$

- The value of h which minimizes the mid-power sensitivity is selected as *optimal* tuning parameter h^* , that is

$$h^* = \arg \min_h \{\delta_{mid}(h)\}.$$

From a practical point of view, it is fundamental to identify the family of alternative distributions. We consider target alternatives defined as $F_\delta = F_\delta(\hat{\boldsymbol{\mu}}, \hat{\boldsymbol{\Sigma}}, \hat{\boldsymbol{\lambda}})$, where $\hat{\boldsymbol{\mu}}$, $\hat{\boldsymbol{\Sigma}}$ and $\hat{\boldsymbol{\lambda}}$ indicate the location, covariance and skewness parameter estimates from the pooled sample. The implementation of the described procedure is reported in Algorithm 2.

Algorithm 2 Algorithm to select optimal h

- 1: Compute the estimates of mean $\hat{\boldsymbol{\mu}}$, covariance matrix $\hat{\boldsymbol{\Sigma}}$ and skewness $\hat{\boldsymbol{\lambda}}$ from the pooled sample.
 - 2: Choose the family of alternatives $F_\delta = F_\delta(\hat{\boldsymbol{\mu}}, \hat{\boldsymbol{\Sigma}}, \hat{\boldsymbol{\lambda}})$.
 - 3: **for** δ **do**
 - 4: **for** h **do**
 - 5: Generate $\mathbf{X}_1, \dots, \mathbf{X}_{K-1} \sim F_0$, for $\delta = 0$;
 - 6: Generate $\mathbf{X}_K \sim F_\delta$;
 - 7: Compute the k -sample test statistic between $\mathbf{X}_1, \mathbf{X}_2, \dots, \mathbf{X}_K$ with kernel parameter h ;
 - 8: Repeat lines 5-7 N times.
 - 9: Compute the power of the test. If it is greater than 0.5, select h as optimal value.
 - 10: **end for**
 - 11: **end for**
 - 12: If an optimal value has not been selected, choose the h which corresponds to maximum power.
-

The presented algorithm is available in the `QuadratiK` package [Saraceno et al., 2024]. In particular, it is automatically performed when the tuning parameter h is not provided by the user for the k -sample test, or as the standalone function `select_h`. The implementation of the algorithm offers: (i) *location* alternatives, $F_\delta = SN_d(\hat{\mu} + \delta, \hat{\Sigma}, \hat{\lambda})$, with $\delta = 0.2, 0.3, 0.4$; (ii) *scale* alternatives, $F_\delta = SN_d(\hat{\mu}, \hat{\Sigma} * \delta, \hat{\lambda})$, $\delta = 0.1, 0.3, 0.5$; (iii) *skewness* alternatives, $F_\delta = SN_d(\hat{\mu}, \hat{\Sigma}, \hat{\lambda} + \delta)$, with $\delta = 0.2, 0.3, 0.6$. The values of $h = 0.6, 1, 1.4, 1.8, 2.2$ and $N = 50$ are set as default values. However, the function `select_h` allows the user to set the values of δ and h for a more extensive grid search. It is suggested to follow this approach when computational resources permit.

5 Simulation Study

In this section, we conduct a simulation study to investigate the performance of the proposed multivariate k -sample KBQD tests. The aim of the simulation is the study of the performance characteristics of the proposed tests vis a vis the performance of the maximum mean discrepancy and other existing k -sample and two-sample tests. The comparisons encompass the performance in term of level and power, as well as computational time. In order to evaluate the performance in terms of level, we generate data under the null hypothesis, which posits that all samples are drawn from the same distribution. To assess the power performance, one of the samples is generated from the family of alternative distributions. The test statistics are based on kernels, and an important step in the computation is the selection of the kernel tuning parameter. We consider $h = 0.2(0.4)10$. The smallest value of h which yields power greater than or equal to 0.5 is selected as optimal, according to the procedure described in Section 4.1. All simulations were performed using R 4.2.0 on the computing resources located at the State University of New York at Buffalo. The implementation of the proposed kernel-based tests can be found in the `QuadratiK` package [Saraceno et al., 2024], both in R and Python.

5.1 Two-sample problem

The proposed two-sample KBQD tests are compared with the existing multivariate two-sample tests. Our preference is selecting the two-sample tests with readily accessible implementations. These include the Friedman-Rafsky Kolmogorov-Smirnov test (FR-KS), the modified Friedman-Rafsky Kolmogorov-Smirnov test (mod-FR-KS), the Friedman-Rafsky Wald-Wolfowitz test (FR-WW), Rosenbaum’s Cross Match test (Crossmatch), the energy test and the Maximum Mean Discrepancy (MMD). Table 1 reports the mentioned two-sample tests and the corresponding R packages.

Table 1: Considered two-sample tests and corresponding R packages.

Test	R package
Crossmatch	<code>crossmatch</code>
Friedman-Rafsky Kolmogorov-Smirnov (FR-KS)	<code>GSAR</code>
modified FR-KS	<code>GSAR</code>
Friedman-Rafsky Wald-Wolfowitz (FR-WW)	<code>GSAR</code>
Energy statistics	<code>energy</code>
Minimum Mean Discrepancy (MMD)	<code>kernalb</code>

The simulation study presented in section 4 shows that the proposed test statistics, trace and T_n , have almost identical performance. Therefore, we will present the results for the T_n statistic, with the MMD and the energy statistics used for comparison. Complete results, including all the considered tests, are reported in section S5 of the Supplementary Material.

In this study, we focus on the family of asymmetric alternatives. More specifically, we generate samples from skew-normal distributions, denoted as $SN_d(\boldsymbol{\mu}, \boldsymbol{\Sigma}, \lambda)$ with location vector $\boldsymbol{\mu}$, covariance matrix $\boldsymbol{\Sigma}$ and shape parameter λ , as introduced by Azzalini and Dalla Valle [1996]. The multivariate skew-normal distribution represents a mathematically tractable extension of the multivariate normal density, with the additional parameter λ to regulate the skewness. When $\lambda = 0$, this corresponds to the multivariate normal. Hill and Dixon [1982] offer a discussion and numerical evidence supporting the presence of skewness in real data. We generate $\boldsymbol{x}_1, \dots, \boldsymbol{x}_{n_1} \sim N_d(\mathbf{0}, \mathbf{I}_d)$ and $\boldsymbol{y}_1, \dots, \boldsymbol{y}_{n_2} \sim SN_d(\mathbf{0}, \mathbf{I}_d, \boldsymbol{\lambda})$, and consider the following three simulation scenarios.

- **Scenario 1:** $d = 1, 2, 6$, sample size $n_1 = n_2 = 100, 500, 1000$, number of replications $N = 1000$, and $\boldsymbol{\lambda} = \lambda \mathbf{1}$ where $\mathbf{1}$ is a vector of ones.
- **Scenario 2:** $d = 20, 50$, sample size $n_1 = n_2 = 500, 1000, 3000$, $N = 100$, and $\boldsymbol{\lambda} = \lambda \mathbf{1}$.
- **Scenario 3:** $d = 4, 7$, sample size $n_1 = n_2 = 50, 100, 500$, $N = 1000$, and $\boldsymbol{\lambda} = (\lambda, 0, \dots, 0)$.

We considered $\lambda = 0, 0.05, 0.1, 0.2, 0.3$.

We start measuring the performance of the proposed kernel-based tests in terms of achieved level when testing the null hypothesis $H_0 : F = G = N_d(\mathbf{0}, \mathbf{I}_d)$. Figure 6 illustrates the level of the KBQD two-sample tests as a function of the tuning parameter

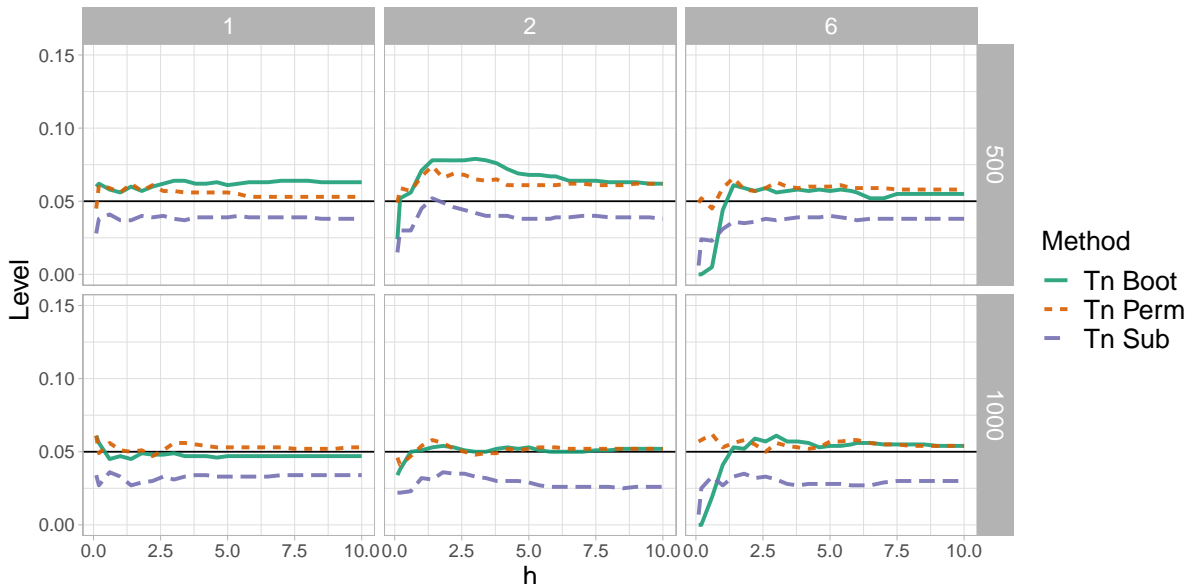


Figure 6: Scenario 1: Level of kernel-based quadratic distance test T_n , with critical value computed using Bootstrap, Permutation and Subsampling, as function of the tuning parameter h , for the combinations of dimension $d = 1, 2, 6$ and sample size $n = 500, 1000$, indicated as headers.

h , using the three different sampling methods to calculate the empirical critical value. The horizontal line in these plots indicates the theoretical level $\alpha = 0.05$. In Figure 7,

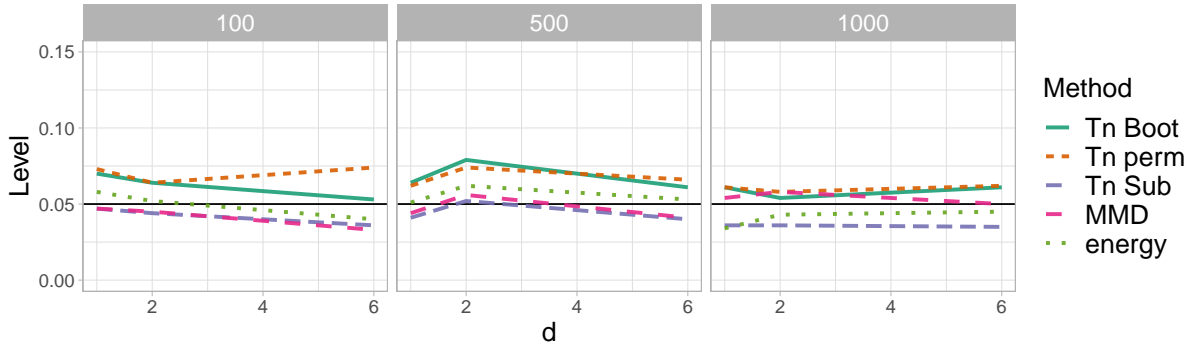


Figure 7: Scenario 1: Level of kernel-based quadratic distance tests, with critical value computed using Bootstrap, Permutation and Subsampling, compared to the MMD and energy tests with respect to the dimension d and sample size n indicated as header. The tuning parameter of the KBQD tests is obtained via algorithm 2.

we compare the level of the considered two-sample tests with respect to the sample size n and the dimension d , against MMD and the energy tests. The tuning parameter of the tests is obtained via the use of algorithm 2. Figure 6 indicates that the achieved level of KBQD tests is very close to the theoretical value for almost all h across different values of n and d . The subsampling algorithm achieves a level lower than the nominal. The level of kernel-based test with subsampling remains quite consistent, whereas it is slightly higher than the nominal level for the tests obtained via the permutation and bootstrap algorithms.

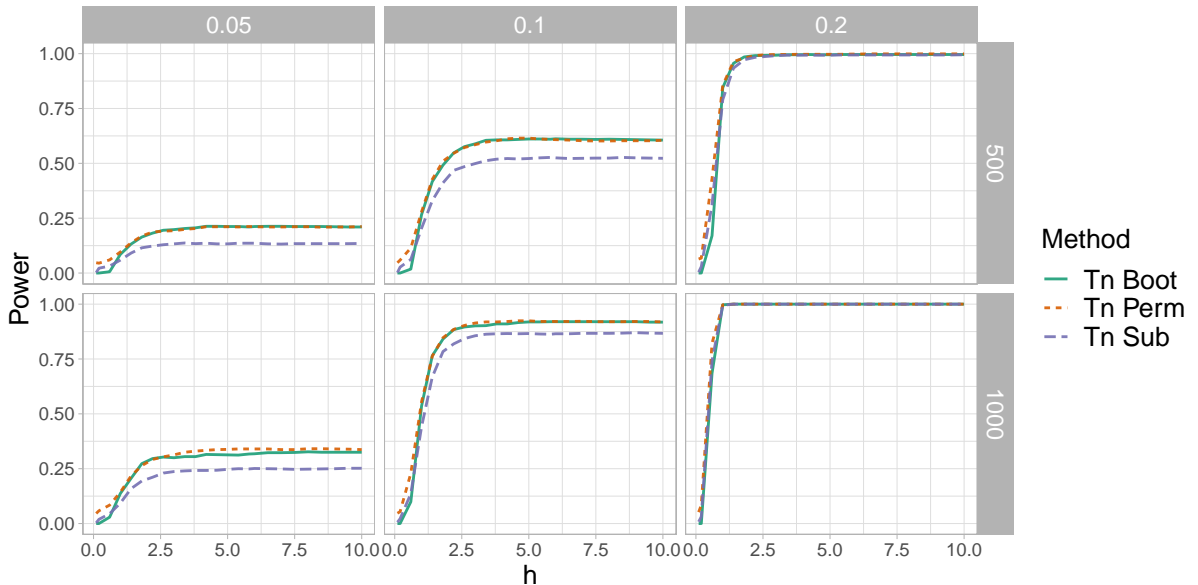


Figure 8: Scenario 1: Power of kernel based test statistic T_n , with the critical value computed using bootstrap, permutation and subsampling, as function of h . $\lambda = 0.05, 0.1, 0.2$, $d = 6$ and $n = 500, 1000$.

We next compare the power performance of the kernel-based test with respect to the value of h and against the existing multivariate two-sample goodness-of-fit tests. Figure

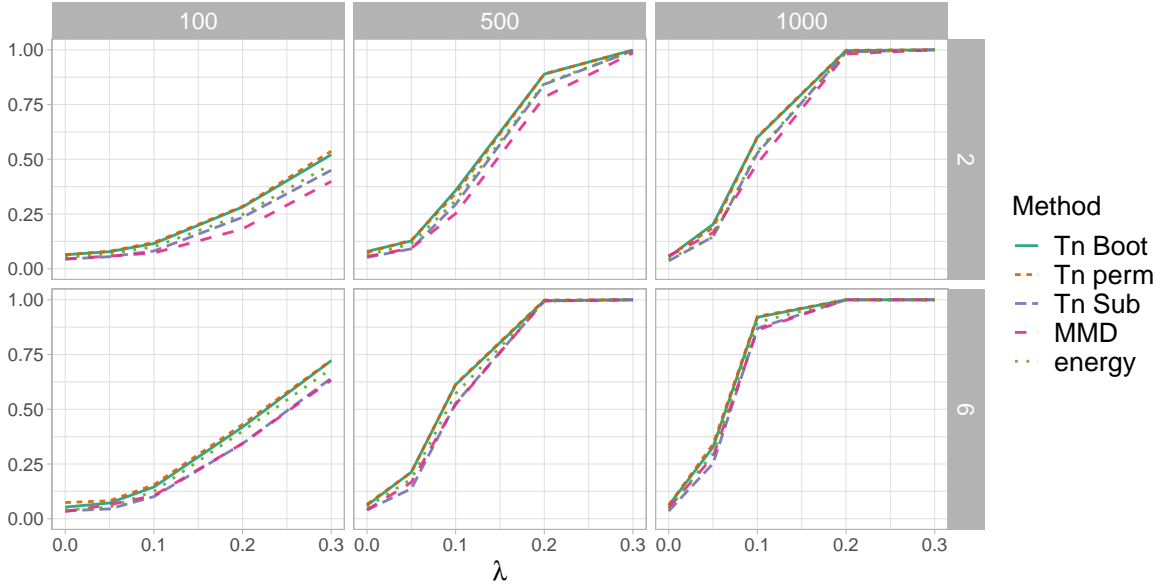


Figure 9: Scenario 1: Power of kernel based test T_n , with the critical value computed using bootstrap, permutation and subsampling, compared with MMD and energy tests as function of λ for sample size n and dimension d , indicated as headers on the x -axis and y -axis respectively. The tuning parameter of the KBQD tests is obtained via algorithm 2.

8 shows the power of the proposed tests as a function of the tuning parameter h for different values of the skewness parameter λ , $d = 6$ and $n = 500, 1000$. If subsampling is used the test achieves slightly lower power for alternatives closer to the null, while it performs similarly to the bootstrap and permutation algorithms when λ increases. Figure 9 illustrates the power of the proposed KBQD tests in comparison with the MMD and energy tests, with respect to the skewness parameter λ , for different dimensions and sample sizes, indicated as headers. It is evident that as the skewness of the distributions increases, so does the power across all the tests being investigated. The KBQD tests consistently demonstrate enhanced power performance compared to the MMD and energy tests. In particular, the KBQD test with subsampling shows a performance akin to the MMD test and energy tests for $d > 1$, while for $d = 1$ it outperforms the MMD test. The KBQD tests with permutation and bootstrap outperform all others, especially for smaller dimensions or sample size. Simulation results for $d = 1$ are available in Section S5 of the Supplemental Material. The Crossmatch, FR-WW and FR-KS two-sample tests exhibit a poor performance against asymmetric alternatives, with the exception of the FR-KS which is competitive in the univariate case. KBQD tests are competitive together with the MMD and energy tests, while outperform the remaining tests.

The second simulation scenario investigates the performance of the two-sample tests in a higher dimensional setting. Figure 10 shows the power of the proposed tests as a function of the tuning parameter h for different values of the skewness parameter λ , $d = 20$ and $n = 500, 3000$. As in the previous scenario, higher values of h obtain higher power. Figures 11 and 12 illustrate the level and the power of the proposed KBQD test T_n in comparison to the MMD and energy tests, with respect to the skewness parameter λ , for the considered values of dimension d and sample size. The level of the proposed tests fluctuates around the nominal $\alpha = 0.05$ level, with T_n based on the bootstrap method

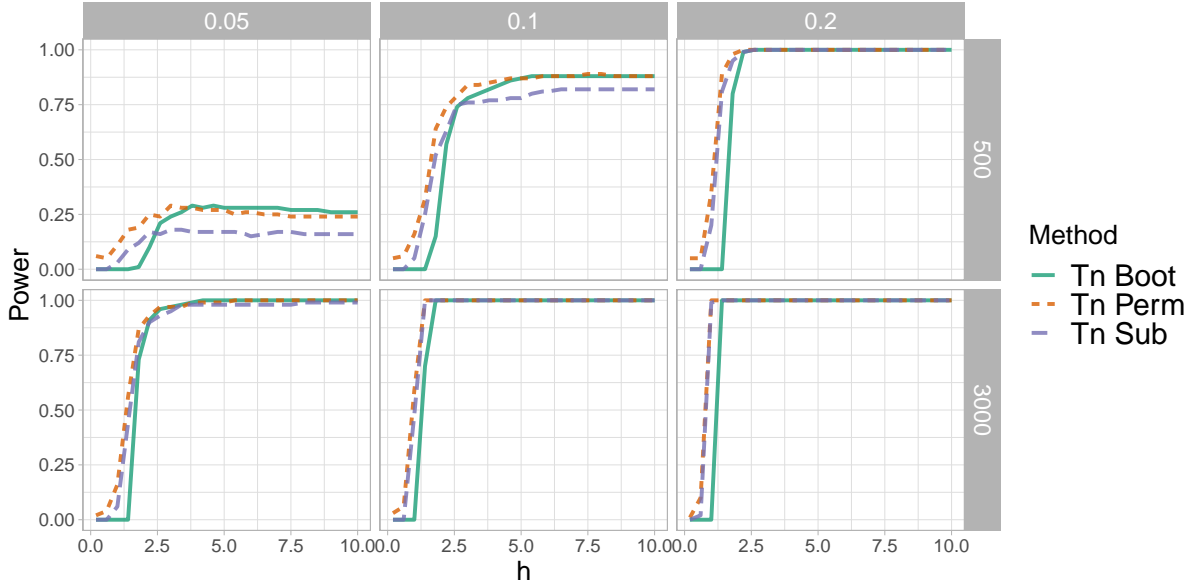


Figure 10: Scenario 2: Power of KBQD test T_n , with the critical value computed using bootstrap, permutation and subsampling, as function of h for $d = 20$. The sample size $n = 500, 3000$ and $\lambda = 0.05, 0.1, 0.3$ are indicated as headers.

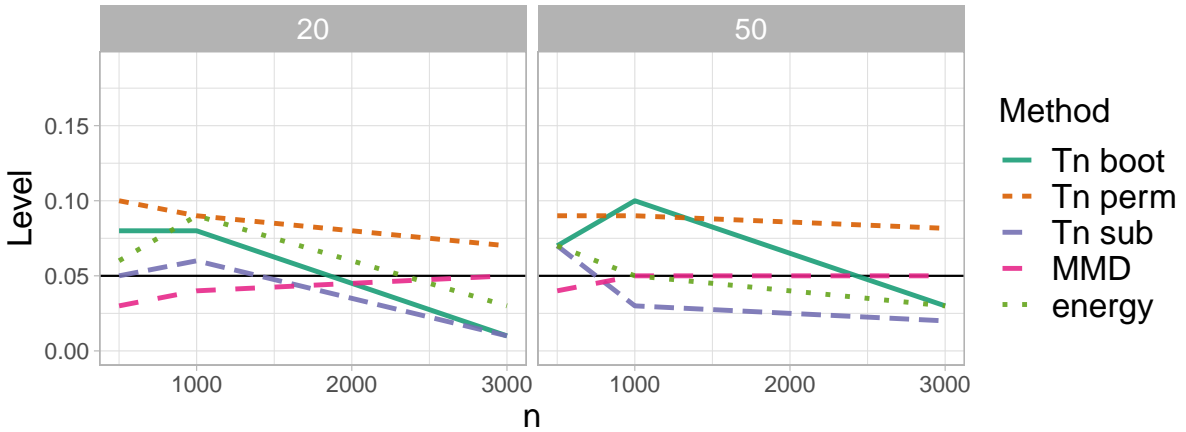


Figure 11: Scenario 2: Level KBQD test T_n , with the critical value computed using bootstrap, permutation and subsampling, compared with the MMD and energy tests, for dimension $d = 20, 50$ and sample size $n = 500, 1000, 3000$. The tuning parameter of the KBQD tests is obtained via algorithm 2.

becoming conservative as the sample size increases, a trend that is followed by the energy test as well. In terms of power, the KBQD tests achieve competitive results when the sample size and the dimension increase, and show a power enhancement for small sample sizes with respect to the dimension. The Crossmatch, FR-WW and FR-KS tests have a poor performance in terms of both level and power.

The simulation results for the third scenario show that the proposed two-sample tests have similar performances, and details are reported in Section S5 of the Supplemental Material.

Finally, the considered two-sample tests are compared in terms of computational time. We generate $N = 100$ samples from a d -dimensional standard normal distribution

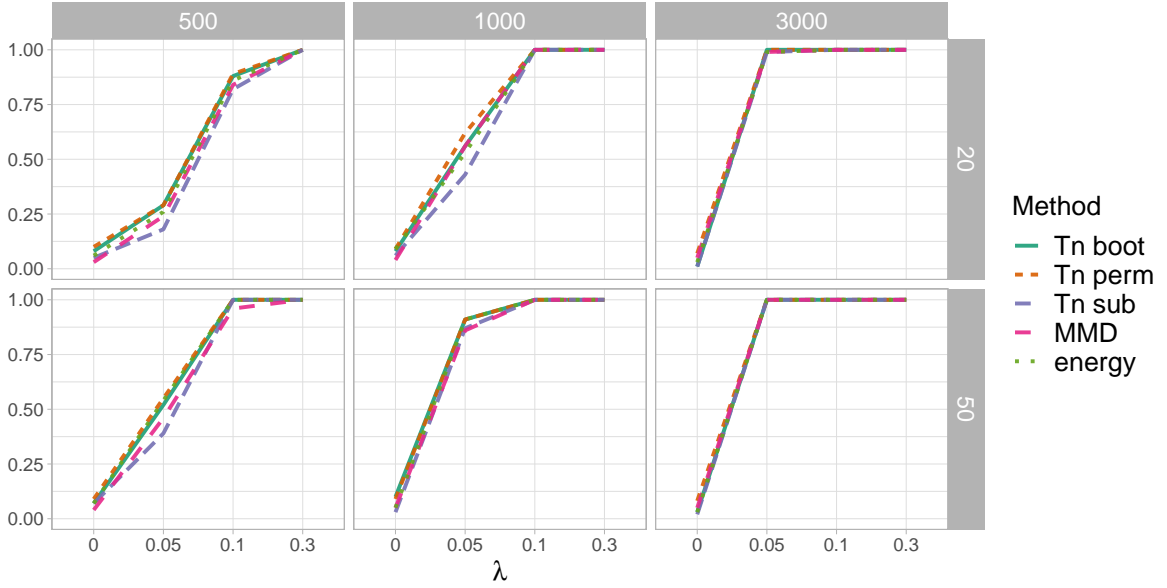


Figure 12: Scenario 2: Power of KBQD test T_n , with the critical value computed using bootstrap, permutation and subsampling, compared with the MMD and energy tests, for dimension $d = 20, 50$ and sample size $n = 500, 1000, 3000$ indicated as headers. The tuning parameter of the KBQD tests is obtained via algorithm 2.

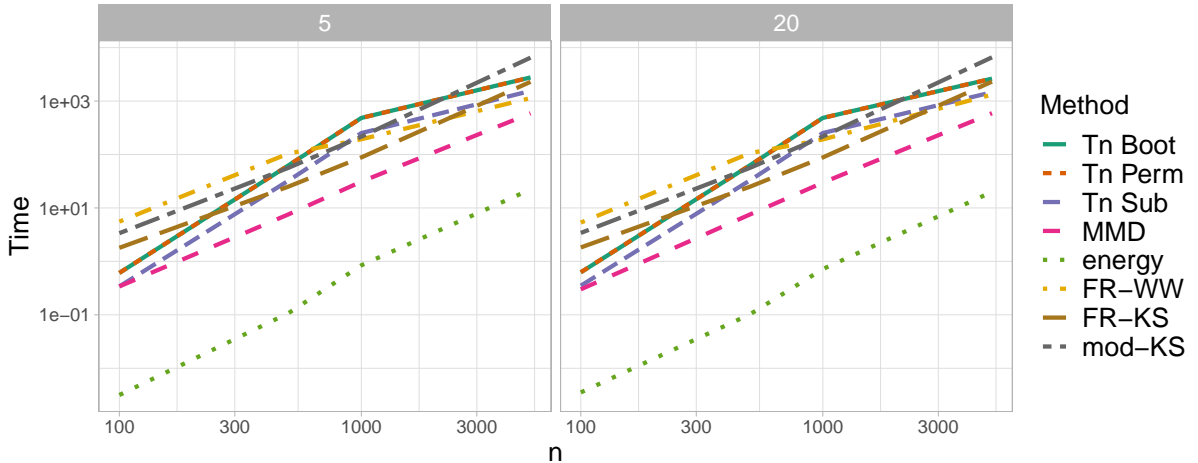


Figure 13: Computational time (in log scale) needed by the considered two-sample tests, as function of the sample size n for dimension $d = 5, 20$.

with $d = 5, 20$ and sample size $n = 100, 500, 1000, 5000$. The KBQD tests, energy and MMD tests are computed using $B = 150$ replications. Figure 13 shows the average computational time (in logarithmic scale) used by the considered two-sample tests. The KBQD tests with subsampling exhibits the same time as MMD. The energy test is the fastest and outperforms all tests in terms of computational time.

Additional asymmetric distributions

We further investigate the performance of the introduced KBQD tests against asymmetric alternatives by considering additional skewed distributions, that is the log-normal distribution $\log N(\mu, \sigma)$ and the Gumbel distribution $\text{Gumbel}(\mu, \sigma)$, where μ and σ de-

note the location and scale parameters, respectively. We generate univariate observations according to the following scenarios.

- **Log-normal:** $\mathbf{x}_1, \dots, \mathbf{x}_{n_1} \sim \log N(0, 0.8)$ and $\mathbf{y}_1, \dots, \mathbf{y}_{n_2} \sim \log N(0, \sigma)$ with $\sigma = 0.6, 0.65, 0.7, 0.75, 0.8$.
- **Gumbel-scale:** $\mathbf{x}_1, \dots, \mathbf{x}_{n_1} \sim \text{Gumbel}(0, 1)$ and $\mathbf{y}_1, \dots, \mathbf{y}_{n_2} \sim \text{Gumbel}(0, \sigma)$ with $\sigma = 0.8, 0.9, 1, 1.1, 1.2$.
- **Gumbel-location:** $\mathbf{x}_1, \dots, \mathbf{x}_{n_1} \sim \text{Gumbel}(0, 1)$ and $\mathbf{y}_1, \dots, \mathbf{y}_{n_2} \sim \text{Gumbel}(\mu, 1)$ with $\mu = 0, 0.1, 0.2, 0.3$.

The sample size is $n_1 = n_2 = 50, 100, 500$, $B = 150, 300, 500$, and the number of replications $N = 1000$. For these cases, we compare the KBQD tests only with MMD and energy tests, considering the poor performance of the other tests in the previous simulations. The performance of the KBQD tests with respect to the tuning parameter h is consistent with previous results. In terms of power, the proposed tests with the bootstrap and permutation algorithms show an increased power for all the considered scenarios. Complete results are reported in Section S4 of the Supplemental Material.

5.2 k -sample problem

We investigate the performance of the k -sample KBQD tests in the case of k samples. The existing multivariate k -sample tests are considered for analyzing the differences with the proposed tests. The literature includes few multivariate k -sample tests with a readily available implementation. In this simulation study, we include the k -sample energy test and the independence k -sample tests, available in the `Python` package `hyppo`. In particular, we consider the tests with the MMD and the energy test as Independence tests. The `KSample` function in the `hyppo` package is performed using as independence tests the distance correlation `DCorr`, which is equivalent to the k -sample Energy test, and the Hilbert-Schmidt independence criterion `Hsic`, which corresponds to the MMD.

Bivariate example with normal distribution

We consider the hypothesis testing problem $H_0 : F_1 = F_2 = F_3$ with $F_i \sim N_2(\boldsymbol{\mu}, \mathbf{I}_2)$ follows a bivariate normal distribution with mean vector $\boldsymbol{\mu}$. We distinguish three cases.

- **None:** The three samples are generated from the same normal distribution with $\boldsymbol{\mu} = (0, 0)$.
- **One:** Two samples are generated from the standard normal distribution, and $F_3 \sim N_2(\boldsymbol{\mu}, \mathbf{I}_2)$ with $\boldsymbol{\mu} = (0, \epsilon)$.
- **All:** The three samples are generated from different normal distributions with mean vectors $\boldsymbol{\mu}_1 = (0, \sqrt{3}/3 \times \epsilon)$, $\boldsymbol{\mu}_2 = (-\epsilon/2, -\sqrt{3}/6 \times \epsilon)$ and $\boldsymbol{\mu}_3 = (\epsilon/2, -\sqrt{3}/6 \times \epsilon)$.

For all these cases, we consider sample size $n_1 = n_2 = 100, 200, 500$, $\epsilon = 0, 0.1, \dots, 1$, $B = 150$ and $N = 1000$ replications. Figure 14 shows the level of the KBQD test compared to the energy test and the independence tests, in the **None** case, in which the null hypothesis is true. The power achieved by the considered tests is displayed in Figure 15 for the other two cases and different sample sizes. The proposed KBQD tests, with

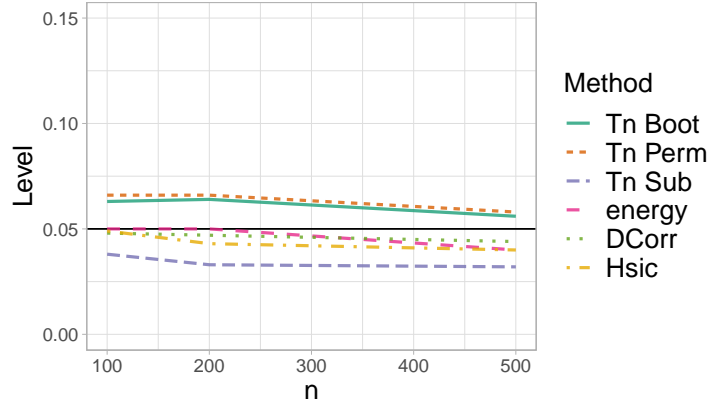


Figure 14: Normal distribution: Level of the KBQD test T_n , with the critical value computed using bootstrap, permutation and subsampling, compared with the available k -sample tests, as function of sample size n and $d = 2$. The black line corresponds to the nominal level 0.05.

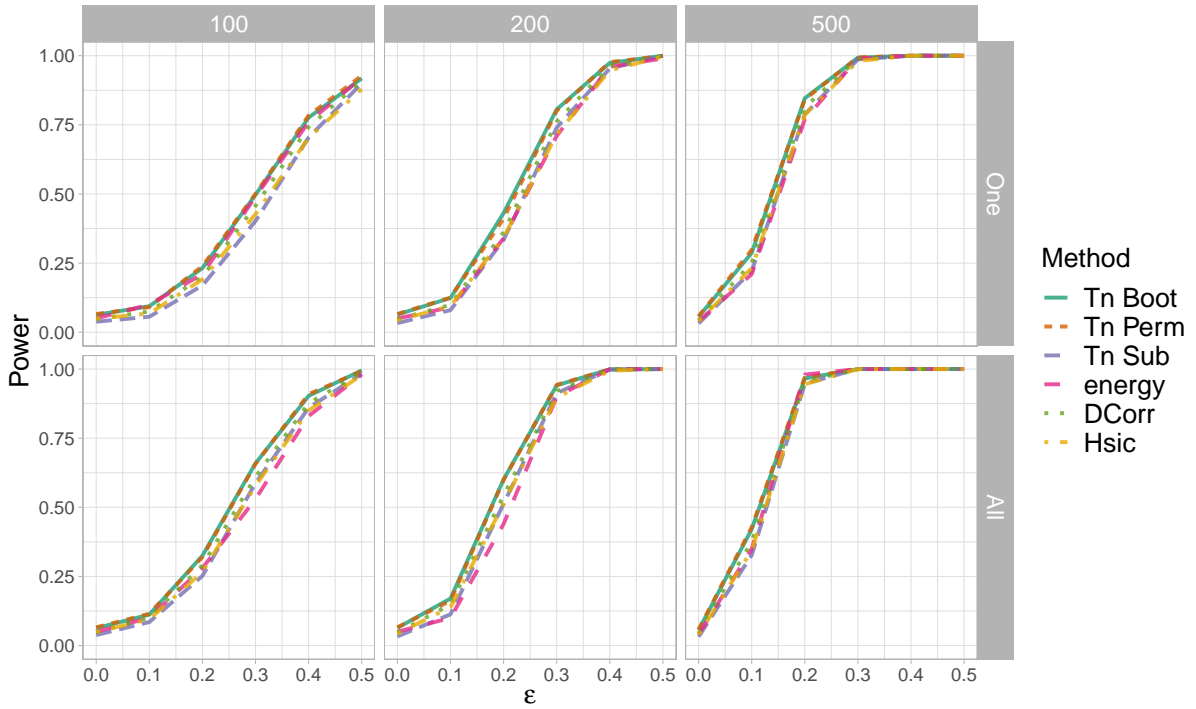


Figure 15: Normal distribution: Power of the KBQD test T_n , with the critical value computed using bootstrap, permutation and subsampling, as function of ϵ for sample size $n = 100, 200, 500$ indicated as column headers. The simulation scenario is indicated as row header. We display here $\epsilon \in [0, 0.5]$.

bootstrap and permutation algorithms, show higher power than the other tests especially for lower sample size and small departures from the null hypothesis, maintaining a level close to the nominal one. The KBQD test with the subsampling algorithm shows similar performance to the MMD.

Additional alternative distributions

We focus now on families of alternative distributions different from the Gaussian distribution. More specifically, we generate $k - 1$ samples according to the null hypothesis, and the remaining sample from the family of alternatives indexed by ϵ . The following alternatives are taken into consideration.

- **Cauchy distribution:** One sample is generated from the d -variate Cauchy distribution, that is $F_1 \sim \text{Cauchy}(\boldsymbol{\epsilon}, \mathbf{I}_d)$, while $F_i \sim \text{Cauchy}(\mathbf{0}, \mathbf{I}_d)$, for $i \neq 1$.
- **t -distribution:** One sample is generated from the d -variate t distribution with 4 degrees of freedom, that is $F_1 \sim t_4(\boldsymbol{\epsilon}, \mathbf{I}_d)$, while $F_i \sim t_4(\mathbf{0}, \mathbf{I}_d)$, for $i \neq 1$.

We consider $k = 3, 5$ number of samples, $B = 150$, $N = 1000$, $n = 50, 200, 500$ per sample with $d = 2, 6, 10$, and additionally $n = 1000$ when $d = 10$. For each family of distributions, we consider two types of alternatives:

Type 1: $\boldsymbol{\epsilon}$ is a d -dimensional constant vector, that is $\boldsymbol{\epsilon} = (\epsilon, \dots, \epsilon)$.

Type 2: $\boldsymbol{\epsilon}$ has the first half elements equal to ϵ and the remaining equal to zero.

We report here the simulation results for alternatives following the Cauchy distribution, while the results for the t -distribution can be found in Section S5 of the Supplementary Material.

Figure 16 depicts the level obtained by the KBQD tests, the energy test and the independence tests when testing the equality of samples from Cauchy distributions as function of the sample size n , for different values of dimension d and number of samples k . Figure 17 compares the performance of the k -sample tests in terms of power as function of ϵ , for **Type 2** alternatives and $k = 5$ samples, considering different values of dimension d and sample size (per sample) n .

The KBQD tests with the bootstrap and permutation algorithms show slightly higher level than the nominal one. On the other hand, using the subsampling algorithm, the level is lower, and approaches the nominal level for higher dimensions and increasing sample size. Figure 17 shows that the proposed KBQD tests outperform the available k -sample tests, especially for higher dimensions and small sample sizes. The Independence test *Hsic* is competitive only for dimension $d = 2$.

5.3 Real data application

Here, we consider the Palmer Archipelago (Antartica) penguin dataset, originally collected by Gorman et al. [2014] and made available in the R package `palmerpenguins` [Horst et al., 2020]. This data set contains complete measurements of 4 continuous variables for 342 penguins, which belong to 3 different species and they were collected from 3 islands in the Palmer Archipelago, Antartica.

For each variable, Figure 18 displays the estimated density, boxplot and histogram and bi-variate scatter plots colored by species. The boxplots and histograms show that penguins from the three species present differences with respect to the considered characteristics. In particular, according the estimated densities, the "Adelie" and "Chinstrap" species appear to follow similar distributions in all the variables except for the "Bill Length". In fact, from the bivariate scatter plots, the species are well separated when "Bill Length" is considered together with another variable.

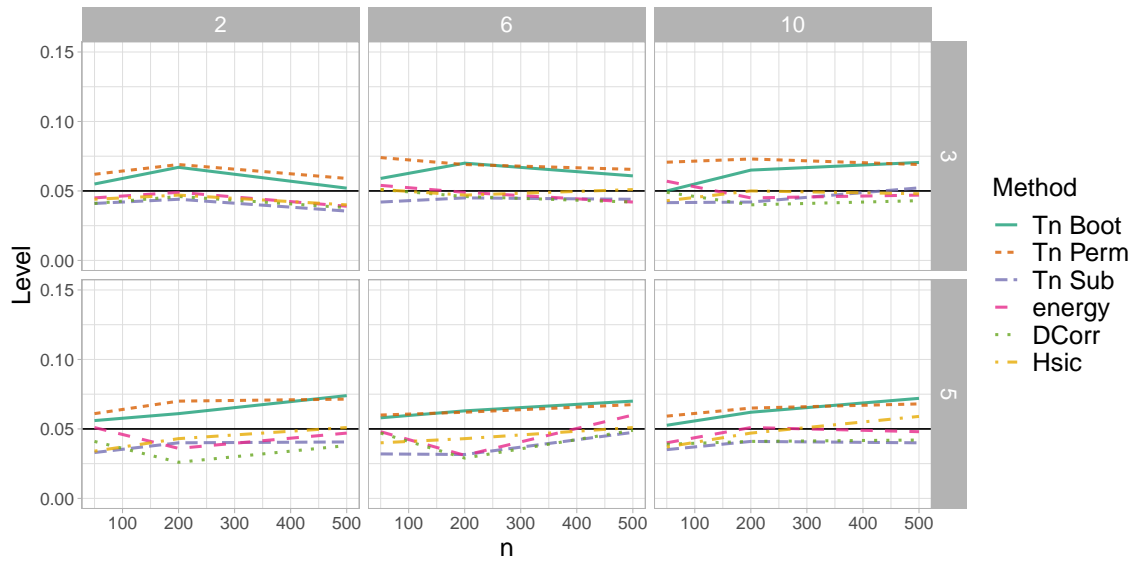


Figure 16: Cauchy distribution: Level of KBQD test T_n , with the critical value computed using bootstrap, permutation and subsampling, compared with the available k -sample tests, as function of sample size n , for dimension $d = 2, 6, 10$ and number of samples $k = 3, 5$ indicated as headers. The black line indicates the nominal level 0.05.

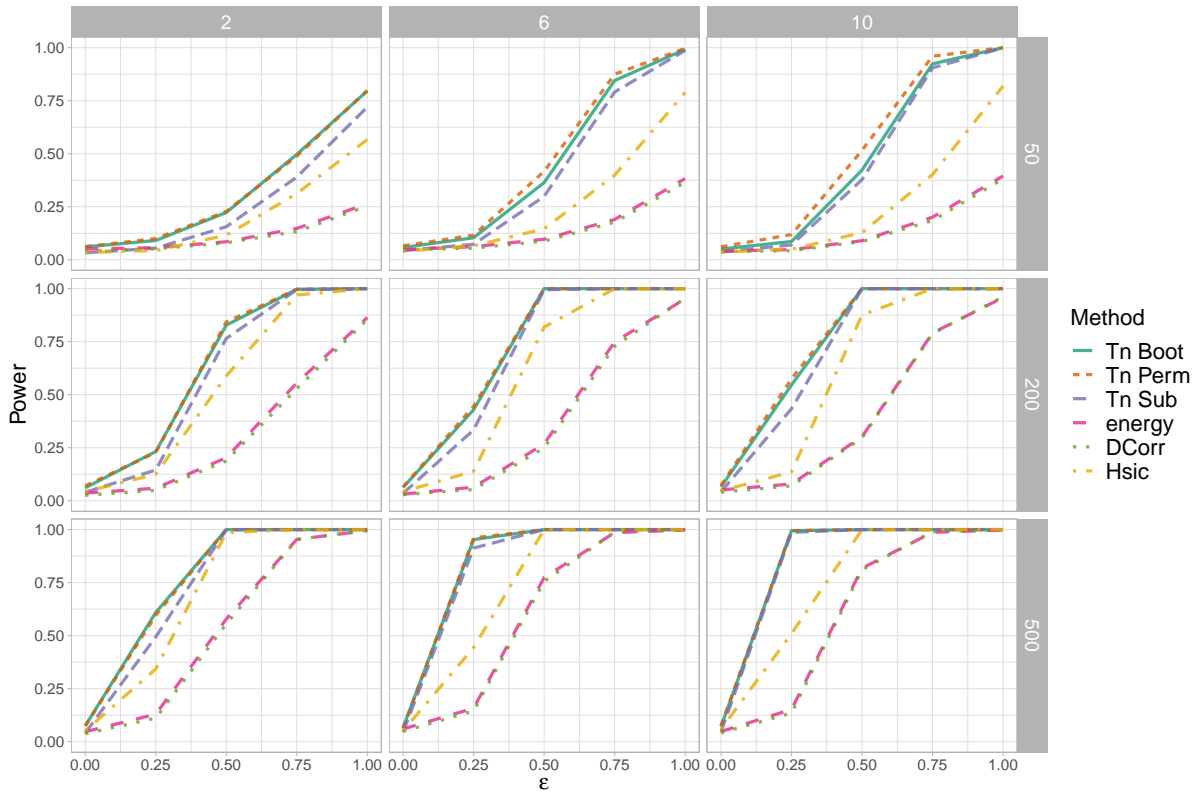


Figure 17: Cauchy distribution: Power of KBQD test T_n , with the critical value computed using bootstrap, permutation and subsampling, compared with the available k -sample tests, as function of ϵ following **Type 2** alternatives, with ϵ from 0 to 1, for sample size per group $n = 50, 200, 500$ and dimension $d = 2, 6, 10$, indicated as headers. The number of samples is $k = 5$.

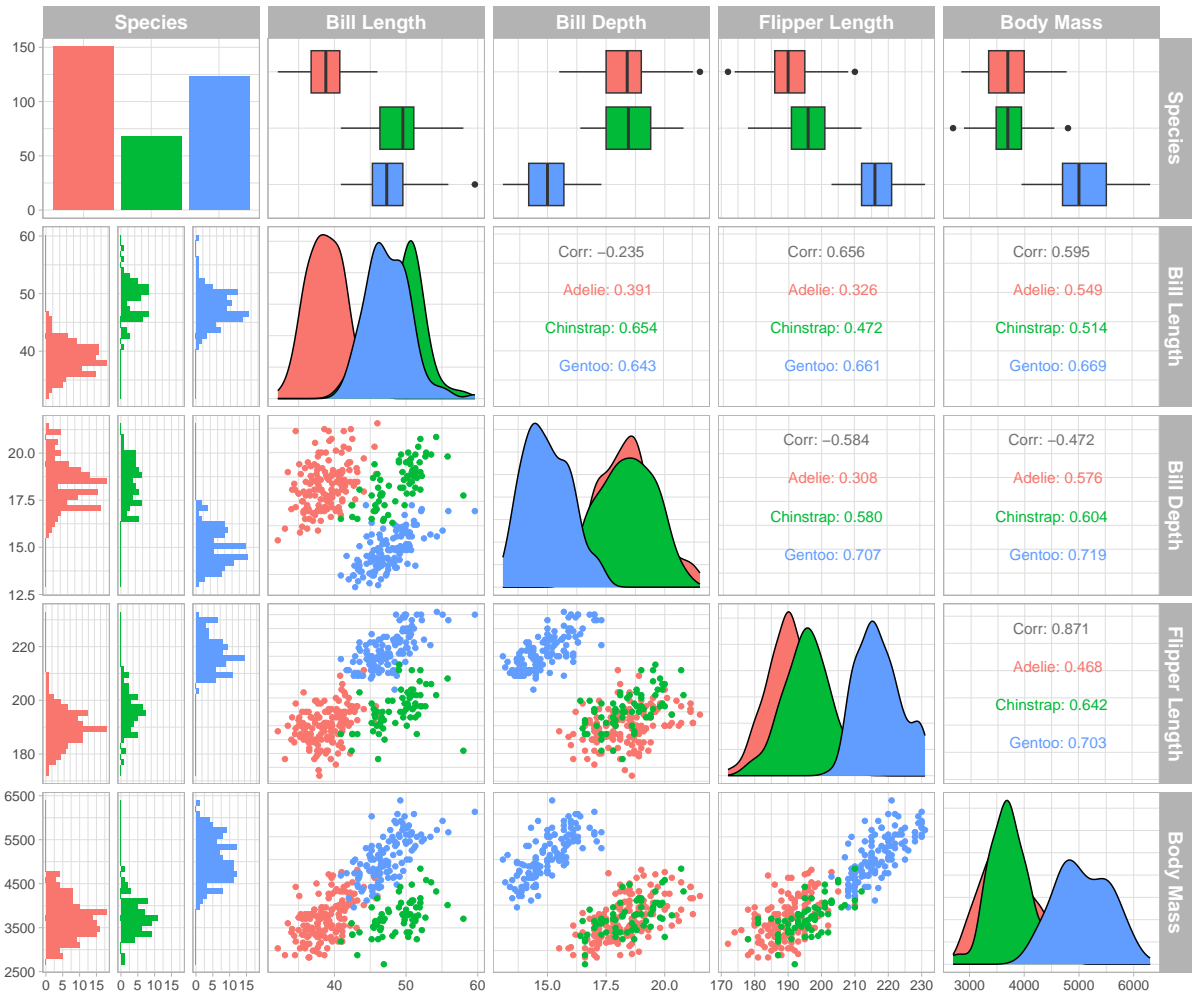


Figure 18: Pairs plots of the variables in the penguin data set. It displays the histogram and boxplots of each variable on the first column and the first row, respectively. On the main diagonal, the estimated densities are showed, while the bivariate scatter plot and pairwise correlations are reported on the off diagonal. In all the plot, the species is indicated with different colors.

At first, we perform the kernel-based quadratic distance k -sample tests and several other competitor tests to assess if the difference between these three groups is significant. All the considered k -sample tests reject the null hypothesis of equality among the groups. Table S2 in section S6 of the Supplemental Material reports the obtained test statistics, critical values and/or p -values. Considering the greater similarity between the "Adelle" and "Chinstrap" species, we want to assess the performance of the two-sample tests when comparing these two groups of observations. The KBQD tests, independently of the sampling algorithm, together with the Friedman-Rafsky Wald-Wolfowitz test and the modified Friedman-Rafsky Kolmogorov-Smirnov test, reject the null hypothesis, while the MMD, the Energy test and KS test do not reject the hypothesis of equality between the two distributions. Table 2 reports the obtained test statistics, the critical value or the p -value, and their answer to the null hypothesis.

Table 2: Results of the considered two-sample tests when comparing the "Adelie" and "Chinstrap" species of the Penguin data set. For each test, the obtained test statistic, the critical value or the p -value, and the final answer to the null hypothesis are displayed. The KBQD tests are performed with the indicated h , selected via algorithm 2.

Method	h	Statistics	critical Value	p-value	reject H_0
Tn Sub	0.8	1.346008	0.9243748	-	TRUE
Tn Boot	1.6	2.802167	2.598121	-	TRUE
Tn Perm	0.8	1.346008	0.7078004	-	TRUE
MMD	-	0.0127364	0.0288944	-	FALSE
energy	-	671.89	-	0.1788	FALSE
FR-WW	-	-7.705333	-	0.0010	TRUE
FR-KS	-	0.9636135	-	0.2587413	FALSE
mod-KS	-	-23.15271	-	0.015984	TRUE

6 Conclusions

In this paper we present a unified framework for the study of goodness of fit that is based on the concept of matrix distance. Specifically, we define the kernel-based matrix distance and associated statistics for testing equality of distributions in k -samples. We show that the two-sample goodness-of-fit is a special case of this formulation, and propose algorithms to facilitate the computation of the test statistics. We also discuss the asymptotic distribution of the matrix distance, and thoroughly investigate the performance of the KBQD tests. The performance of the test statistics depends on a kernel tuning parameter h . We propose an algorithm for selecting this parameter and exemplify its use in our simulation, and example, sections. Our simulation results indicate that the proposed tests outperform, in terms of power, the MMD and energy tests for alternatives close to the null hypothesis and for distributions with heavy tails. An example of such distributions is the family of Cauchy(ϵ, I). In summary, the proposed framework allows goodness of fit testing with $k \geq 2$. Furthermore, our proposed tests perform well in terms of level and power. They are at least competitive when compared with the state-of-the-art tests in the literature, and outperform those in terms of power for contiguous alternatives, heavy tailed distributions and in higher dimensions. The proposed tests and algorithms are implemented in the software `QuadratIK` that can be used in both, `R` and `Python` environments.

Appendix A Proofs

A.1 Proof of Proposition 1

Note that

$$\begin{aligned}
d_K(F, G) &= \iiint \mathbf{k}(\mathbf{x}, \mathbf{t}) \mathbf{k}^\top(\mathbf{y}, \mathbf{t}) du(\mathbf{t}) d(F - G)(\mathbf{x}) d(F - G)(\mathbf{y}) \\
&= \iint \left\{ \int \mathbf{k}(\mathbf{x}, \mathbf{t}) \mathbf{k}^\top(\mathbf{y}, \mathbf{t}) du(\mathbf{t}) \right\} dF(\mathbf{x}) dF(\mathbf{y}) \\
&\quad - \iint \left\{ \int \mathbf{k}(\mathbf{x}, \mathbf{t}) \mathbf{k}^\top(\mathbf{y}, \mathbf{t}) du(\mathbf{t}) \right\} dF(\mathbf{x}) dG(\mathbf{y}) \\
&\quad - \iint \left\{ \int \mathbf{k}(\mathbf{x}, \mathbf{t}) \mathbf{k}^\top(\mathbf{y}, \mathbf{t}) du(\mathbf{t}) \right\} dG(\mathbf{x}) dF(\mathbf{y}) \\
&\quad + \iint \left\{ \int \mathbf{k}(\mathbf{x}, \mathbf{t}) \mathbf{k}^\top(\mathbf{y}, \mathbf{t}) du(\mathbf{t}) \right\} dG(\mathbf{x}) dG(\mathbf{y}).
\end{aligned}$$

Let $\mathbf{k}(F, \mathbf{t})$ be a vector with coordinates $\int k_i(\mathbf{x}, \mathbf{t}) dF(\mathbf{x})$ and similarly $\mathbf{k}(G, \mathbf{t})$ the vector with coordinates $\int k_j(\mathbf{y}, \mathbf{t}) dG(\mathbf{y})$. Changing the order of integration by Tonelli's Theorem, we obtain the following

$$\begin{aligned}
d_K(F, G) &= \int \mathbf{k}(F, \mathbf{t}) \mathbf{k}^\top(F, \mathbf{t}) du(\mathbf{t}) - \int \mathbf{k}(F, \mathbf{t}) \mathbf{k}^\top(G, \mathbf{t}) du(\mathbf{t}) \\
&\quad - \int \mathbf{k}(G, \mathbf{t}) \mathbf{k}^\top(F, \mathbf{t}) du(\mathbf{t}) + \int \mathbf{k}(G, \mathbf{t}) \mathbf{k}^\top(G, \mathbf{t}) du(\mathbf{t}) \\
&= \int (\mathbf{k}(F, \mathbf{t}) - \mathbf{k}(G, \mathbf{t})) (\mathbf{k}(F, \mathbf{t}) - \mathbf{k}(G, \mathbf{t}))^\top du(\mathbf{t}),
\end{aligned}$$

and $d_K(F, G) = d_K(G, F)$, therefore $d_K(F, G)$ is symmetric.

A.2 Proof of Proposition 2

Under the null hypothesis, we have that

$$\int K_{\bar{F}}(\mathbf{s}, \mathbf{t}) d\bar{F}(\mathbf{t}) = \int K_{\bar{F}}(\mathbf{s}, \mathbf{t}) dF_i(\mathbf{t}) = 0 \quad i \in \{1, \dots, k\}.$$

This implies that the centered kernel $K_{\bar{F}}$ has the same eigenvalues and eigenfunctions with respect to F_i , $i \in \{1, \dots, k\}$ under the null hypothesis. Employing the spectral decomposition of the kernel function given by Mercer's Theorem and the uniform convergence theorem, the ij -th element of the distance matrix, with $1 \leq i, j \leq k$, can be written as

$$\begin{aligned}
D_{ij} &= \iint \sum_{p=1}^{\infty} \lambda_p \phi_p(\mathbf{x}) \phi_p(\mathbf{y}) dF_i(\mathbf{x}) dF_j(\mathbf{y}) \\
&= \sum_{p=1}^{\infty} \lambda_p \iint \phi_p(\mathbf{x}) \phi_p(\mathbf{y}) dF_i(\mathbf{x}) dF_j(\mathbf{y}) \\
&= \sum_{p=1}^{\infty} \lambda_p \left(\int \phi_p(\mathbf{x}) dF_i(\mathbf{x}) \right) \left(\int \phi_p(\mathbf{y}) dF_j(\mathbf{y}) \right) \\
&= \sum_{p=1}^{\infty} \lambda_p \bar{\phi}_{p,i} \bar{\phi}_{p,j}.
\end{aligned}$$

A.3 Proof of Proposition 3

From Proposition 2,

$$D_n = \sum_{p=1}^{\infty} \lambda_p \tilde{\phi}_{n,p} \tilde{\phi}_{n,p}^{\top},$$

where $\tilde{\phi}_{n,p}$ has entries given by

$$\bar{\phi}_{n,p,i} = \frac{1}{n_i} \sum_{j=1}^{n_i} \phi_p(\mathbf{x}_j^{(i)}).$$

Note that

$$\mathbb{E}(\bar{\phi}_{n,p,i}) = \frac{1}{n_i} \sum_{j=1}^{n_i} \mathbb{E}(\phi_p(\mathbf{x}_j^{(i)})) = 0,$$

$$\text{Var}(\bar{\phi}_{n,p,i}) = \frac{1}{n_i^2} \left[\sum_{j=1}^{n_i} \mathbb{E}(\phi_p^2(\mathbf{x}_j^{(i)})) + \sum_{j=1}^{n_i} \sum_{\ell \neq j=1}^{n_i} \mathbb{E}(\phi_p(\mathbf{x}_j^{(i)}) \phi_p(\mathbf{x}_\ell^{(i)})) \right] = \frac{1}{n_i},$$

and for $1 \leq i \neq j \leq k$

$$\begin{aligned} \text{Cov}(\bar{\phi}_{n,p,i}, \bar{\phi}_{n,p,j}) &= \mathbb{E} \left[\left(\frac{1}{n_i} \sum_{\ell=1}^{n_i} \phi_p(\mathbf{x}_\ell^{(i)}) \right) \left(\frac{1}{n_j} \sum_{r=1}^{n_j} \phi_p(\mathbf{x}_r^{(j)}) \right) \right] \\ &= \frac{1}{n_i n_j} \sum_{\ell=1}^{n_i} \sum_{r=1}^{n_j} \mathbb{E}(\phi_p(\mathbf{x}_\ell^{(i)}) \phi_p(\mathbf{x}_r^{(j)})) = 0. \end{aligned}$$

Let $\mathbf{A} = \text{diag}(1/n_1, \dots, 1/n_k)$, then, we have that $\mathbf{A}^{-\frac{1}{2}} \tilde{\phi}_{n,p} \xrightarrow{p} N_k(\mathbf{0}, \mathbf{I}_k)$.

Let $\rho_i = \lim_{n, n_i \rightarrow \infty} n_i/n$, with $0 < \rho_i < 1$, and let $\mathbf{V} = \text{diag}(1/\rho_1, \dots, 1/\rho_k)$. Hence, we have that

$$\sqrt{n} \tilde{\phi}_{n,p} = \mathbf{V}^{\frac{1}{2}} \mathbf{A}^{-\frac{1}{2}} \tilde{\phi}_{n,p} \xrightarrow{p} N_k(\mathbf{0}, \mathbf{V}).$$

Finally, this implies that

$$n \hat{\mathbf{D}}_n = \sum_{p=1}^{\infty} \lambda_p n \tilde{\phi}_{n,p} \tilde{\phi}_{n,p}^{\top} \xrightarrow{p} \sum_{p=1}^{\infty} \lambda_p W_p$$

where $W_p \sim \mathcal{W}_k(1, \mathbf{V})$ are independent copies of the Wishart distribution of dimension k , one degree of freedom and covariance matrix \mathbf{V} .

A.4 Proof of Proposition 4

Under the null hypothesis, we have that

$$\int K_{\bar{F}}(\mathbf{s}, \mathbf{t}) d\bar{F}(\mathbf{t}) = \int K_{\bar{F}}(\mathbf{s}, \mathbf{t}) dF_i(\mathbf{t}) = 0.$$

This implies that the centered kernel \bar{F} has the same eigenvalues and eigenfunctions with respect to each F_i under the null hypothesis. By Mercer's theorem, we can write nT_n as

$$\begin{aligned} nT_n &= \sum_{p=1}^{\infty} \lambda_p \left\{ \sum_{i=1}^k \frac{n}{n_i(n_i-1)} \sum_{\ell=1}^{n_i} \sum_{r \neq \ell}^{n_i} \phi_p(\mathbf{x}_\ell^{(i)}) \phi_p(\mathbf{x}_r^{(i)}) \right. \\ &\quad \left. - \frac{2}{k-1} \sum_{i=1}^k \sum_{j>i}^k \frac{n}{n_i n_j} \sum_{\ell=1}^{n_i} \sum_{r=1}^{n_j} \phi_p(\mathbf{x}_\ell^{(i)}) \phi_p(\mathbf{x}_r^{(j)}) \right\}. \end{aligned}$$

Notice that, for $i, j \in \{1, \dots, k\}$

$$\begin{aligned} \sum_{\ell=1}^{n_i} \sum_{r \neq \ell}^{n_i} \phi_p(\mathbf{x}_\ell^{(i)}) \phi_p(\mathbf{x}_r^{(i)}) &= \left(\sum_{\ell=1}^{n_i} \phi_p(\mathbf{x}_\ell^{(i)}) \right)^2 - \sum_{\ell=1}^{n_i} \phi_p^2(\mathbf{x}_\ell^{(i)}), \\ \sum_{\ell=1}^{n_i} \sum_{r=1}^{n_j} \phi_p(\mathbf{x}_\ell^{(i)}) \phi_p(\mathbf{x}_r^{(j)}) &= \left(\sum_{\ell=1}^{n_i} \phi_p(\mathbf{x}_\ell^{(i)}) \right) \left(\sum_{r=1}^{n_j} \phi_p(\mathbf{x}_r^{(j)}) \right), \end{aligned}$$

as well as that $\frac{n}{n_i(n_i-1)}$ is equivalent to n/n_i^2 for large n_i and n . Then, we can further rewrite $n(k-1)T_n$ as

$$\begin{aligned} n(k-1)T_n &= \sum_{p=1}^{\infty} \lambda_p \left\{ (k-1) \sum_{i=1}^k \frac{1}{\rho_i} \left[\left(\frac{1}{\sqrt{n_i}} \sum_{\ell=1}^{n_i} \phi_p(\mathbf{x}_\ell^{(i)}) \right)^2 - \frac{1}{n_i} \sum_{\ell=1}^{n_i} \phi_p^2(\mathbf{x}_\ell^{(i)}) \right] \right. \\ &\quad \left. - 2 \sum_{i=1}^k \sum_{j>i}^k \frac{1}{\sqrt{\rho_i \rho_j}} \left(\frac{1}{\sqrt{n_i}} \sum_{\ell=1}^{n_i} \phi_p(\mathbf{x}_\ell^{(i)}) \right) \left(\frac{1}{\sqrt{n_j}} \sum_{r=1}^{n_j} \phi_p(\mathbf{x}_r^{(j)}) \right) \right\} \\ &= \sum_{p=1}^{\infty} \lambda_p \left\{ \sum_{i=1}^k \sum_{j>i}^k \left(\frac{1}{\sqrt{\rho_i}} \frac{1}{\sqrt{n_i}} \sum_{\ell=1}^{n_i} \phi_p(\mathbf{x}_\ell^{(i)}) - \frac{1}{\sqrt{\rho_j}} \frac{1}{\sqrt{n_j}} \sum_{r=1}^{n_j} \phi_p(\mathbf{x}_r^{(j)}) \right)^2 \right. \\ &\quad \left. - \sum_{i=1}^k \frac{1}{\rho_i} \frac{1}{n_i} \sum_{\ell=1}^{n_i} \phi_p^2(\mathbf{x}_\ell^{(i)}) \right\}. \end{aligned}$$

Employing the Weak Law of Large Numbers and the Lindeberg-Levy Central Limit Theorem, we have that

$$\begin{aligned} \frac{1}{n_i} \sum_{\ell=1}^{n_i} \phi_p^2(\mathbf{x}_\ell^{(i)}) &\xrightarrow{p} 1 \text{ as } n \rightarrow \infty, \\ \frac{1}{\sqrt{n_i}} \sum_{\ell=1}^{n_i} \phi_p(\mathbf{x}_\ell^{(i)}) &\xrightarrow{d} N(0, 1) \text{ as } n \rightarrow \infty. \end{aligned}$$

Furthermore, by the Fubini's theorem we have for each $1 \leq i \neq j \leq k$

$$\text{Cov} \left(\frac{1}{\sqrt{n_i}} \sum_{\ell=1}^{n_i} \phi_p(\mathbf{x}_\ell^{(i)}), \frac{1}{\sqrt{n_j}} \sum_{r=1}^{n_j} \phi_p(\mathbf{x}_r^{(j)}) \right) = 0.$$

Hence

$$n(k-1)T_n \xrightarrow{d} \sum_{p=1}^{\infty} \lambda_p \left[\sum_{i=1}^k \sum_{j>i}^k \left(\frac{1}{\sqrt{\rho_i}} Z_{ip} - \frac{1}{\sqrt{\rho_j}} Z_{jp} \right)^2 - \sum_{i=1}^k \frac{1}{\rho_i} \right] \text{ as } n_i, n \rightarrow \infty,$$

where Z_{1p}, \dots, Z_{kp} are k independent random variables which follow the standard normal distribution.

A.5 Proof of Lemma 1

Recall that $K_{F^*}(\mathbf{s}, \mathbf{t}) = K(\mathbf{s}, \mathbf{t}) - K(\mathbf{s}, F^*) - K(F^*, \mathbf{t}) + K(F^*, F^*)$. Then

$$\begin{aligned} d_{K_{F^*}}(F, G) &= \iint K(\mathbf{s}, \mathbf{t}) dF(\mathbf{s}) dF(\mathbf{t}) - \int K(\mathbf{s}, F^*) dF(\mathbf{s}) - \int K(F^*, \mathbf{t}) dF(\mathbf{t}) \\ &\quad - 2 \iint K(\mathbf{s}, \mathbf{t}) dF(\mathbf{s}) dG(\mathbf{t}) + 2 \int K(\mathbf{s}, F^*) dF(\mathbf{s}) + 2 \int K(F^*, \mathbf{t}) dG(\mathbf{t}) \\ &\quad + \iint K(\mathbf{s}, \mathbf{t}) dG(\mathbf{s}) dG(\mathbf{t}) - \int K(\mathbf{s}, F^*) dG(\mathbf{s}) - \int K(F^*, \mathbf{t}) dG(\mathbf{t}). \end{aligned}$$

The result follows by the symmetry of the kernel function.

Supplementary information

This manuscript is accompanied by a Supplementary Material document, which includes the derivation of the two-sample statistic as a special case, and provides further simulation results that complement the findings presented in the main manuscript.

Acknowledgements

The first author would like to acknowledge KALEIDA Health Foundation award 82114, that supported the work of the second author.

References

- Niall H Anderson, Peter Hall, and D Michael Titterington. Two-sample test statistics for measuring discrepancies between two multivariate probability density functions using kernel-based density estimates. *Journal of Multivariate Analysis*, 50(1):41–54, 1994.
- B Aslan and Gunter Zech. Statistical energy as a tool for binning-free, multivariate goodness-of-fit tests, two-sample comparison and unfolding. *Nuclear Instruments and Methods in Physics Research Section A: Accelerators, Spectrometers, Detectors and Associated Equipment*, 537(3):626–636, 2005.
- A. Azzalini and A. Dalla Valle. The multivariate skew-normal distribution. *Biometrika*, 83(4):715–726, 12 1996. doi: 10.1093/biomet/83.4.715.
- Armando Sosthene Kali Balogoun, Guy Martial Nkiet, and Carlos Ogouyandjou. Kernel based method for the k -sample problem, 2018. URL <https://arxiv.org/abs/1812.00100>.
- Armando Sosthene Kali Balogoun, Guy Martial Nkiet, and Carlos Ogouyandjou. A k -sample test for functional data based on generalized maximum mean discrepancy, 2022.
- Ali S Barakat, Dana Quade, and Ibrahim A Salama. Multivariate homogeneity testing using an extended concept of nearest neighbors. *Biometrical Journal*, 38(5):605–612, 1996.
- Ludwig Baringhaus and Carsten Franz. On a new multivariate two-sample test. *Journal of Multivariate Analysis*, 88(1):190–206, 2004.
- P. J. Bickel. A distribution free version of the smirnov two sample test in the p -variate case. *The Annals of Mathematical Statistics*, 40(1):1–23, 1969. ISSN 0003-4851.
- M. Biswas, M. Mukhopadhyay, and A.K. Ghosh. A distribution-free two-sample run test applicable to high-dimensional data. *Biometrika*, 101(4):913–926, 2014. ISSN 0006-3444.
- Munmun Biswas and Anil K Ghosh. A nonparametric two-sample test applicable to high dimensional data. *Journal of Multivariate Analysis*, 123:160–171, 2014.

- Ricardo Cao and Ingrid Van Keilegom. Empirical likelihood tests for two-sample problems via nonparametric density estimation. *Canadian Journal of Statistics*, 34(1):61–77, 2006. ISSN 0319-5724.
- H. Chen and J.H. Friedman. A new graph-based two-sample test for multivariate and object data. *Journal of the American Statistical Association*, 112(517):397–409, 2017. ISSN 0162-1459.
- Lisha Chen, Winston Wei Dou, and Zhihua Qiao. Ensemble subsampling for imbalanced multivariate two-sample tests. *Journal of the American Statistical Association*, 108(504):1308–1323, 2013.
- Y. Chen and M. Markatou. Kernel tests for one, two, and k-sample goodness-of-fit: state of the art and implementation considerations. *Statistical Modeling in Biomedical Research: Contemporary Topics and Voices in the Field*, pages 309–337, 2020.
- Yang Chen. *Contribution to the Theory and Application of Statistical Distances*. Phd thesis, University at Buffalo, Department of Biostatistics, Buffalo, NY, 2018.
- Y. Ding, M. Markatou, and G. Saraceno. Poisson kernel-based tests for uniformity on the d -dimensional sphere. *Statistica Sinica*, 2023. doi: doi:10.5705/ss.202022.0347.
- V Alba Fernández, MD Jiménez Gamero, and J Muñoz Garcia. A test for the two-sample problem based on empirical characteristic functions. *Computational Statistics & Data Analysis*, 52(7):3730–3748, 2008.
- J.H. Friedman and L.C. Rafsky. Multivariate generalizations of the wald-wolfowitz and smirnov two-sample tests. *The Annals of Statistics*, 7(4):697–717, 1979. ISSN 0090-5364.
- Kristen B. Gorman, Tony D. Williams, and William R. Fraser. Ecological sexual dimorphism and environmental variability within a community of antarctic penguins (genus *pygoscelis*). *PLOS ONE*, 9(3):1–14, 03 2014. doi: 10.1371/journal.pone.0090081. URL <https://doi.org/10.1371/journal.pone.0090081>.
- A. Gretton, K.M. Borgwardt, M.J. Rasch, B. Schölkopf, and A. Smola. A kernel two-sample test. *The Journal of Machine Learning Research*, 13(1):723–773, 2012.
- Peter Hall and Nader Tajvidi. Permutation tests for equality of distributions in high-dimensional settings. *Biometrika*, 89(2):359–374, 2002.
- Zaid Harchaoui, Francis Bach, and Eric Moulines. Testing for homogeneity with kernel fisher discriminant analysis, 2008. URL <https://arxiv.org/abs/0804.1026>.
- N. Henze. A multivariate two-sample test based on the number of nearest neighbor type coincidence. *The Annals of Statistics*, 16(2):772–783, 1988. ISSN 0090-5364.
- MaryAnn Hill and W. J. Dixon. Robustness in real life: A study of clinical laboratory data. *Biometrics*, 38(2):377–396, 1982.
- Zdeněk Hlávka, Marie Hušková, and Simos G Meintanis. Testing serial independence with functional data. *Test*, 30(3):603–629, 2021.

- Allison Marie Horst, Alison Presmanes Hill, and Kristen B Gorman. *palmerpenguins: Palmer Archipelago (Antarctica) penguin data*, 2020. URL <https://allisonhorst.github.io/palmerpenguins/>. R package version 0.1.0.
- Marie Husková and Simos G. Meintanis. Tests for the multivariate k-sample problem based on the empirical characteristic function. *Journal of Nonparametric Statistics*, 20:263 – 277, 2008.
- J. Kiefer. K-sample analogues of the kolmogorov-smirnov and cramer-v. mises tests. *The Annals of Mathematical Statistics*, 30(2):420–447, 1959.
- B.G. Lindsay, M. Markatou, S. Ray, K. Yang, and S-C. Chen. Quadratic distances on probabilities: A unified foundation. *The Annals of Statistics*, 36(2):983–1006, 2008. ISSN 0090-5364.
- B.G. Lindsay, M. Markatou, and S. Ray. Kernels, degrees of freedom, and power properties of quadratic distance goodness-of-fit tests. *Journal of the American Statistical Association*, 109(505):395–410, 2014.
- Zhenyu Liu and Reza Modarres. A triangle test for equality of distribution functions in high dimensions. *Journal of Nonparametric Statistics*, 23(3):605–615, 2011.
- M. Markatou, Y. Chen, G. Afendras, and B.G. Lindsay. *Statistical Distances and Their Role in Robustness*, pages 3–26. Springer International Publishing, Cham, 2017. ISBN 978-3-319-69416-0. doi: 10.1007/978-3-319-69416-0_1.
- C.E. Mitchell, R.D. Ryne, and K. Hwang. Using kernel-based statistical distance to study the dynamics of charged particle beams in particle-based simulation codes. *Phys. Rev. E*, 106:065302, Dec 2022. doi: 10.1103/PhysRevE.106.065302.
- Pronoy K. Mondal, Munmun Biswas, and Anil K. Ghosh. On high dimensional two-sample tests based on nearest neighbors. *Journal of Multivariate Analysis*, 141:168–178, 2015. ISSN 0047-259X.
- C. Radhakrishna Rao. Diversity: Its measurement, decomposition, apportionment and analysis. *Sankhyā: The Indian Journal of Statistics, Series A (1961-2002)*, 44(1):1–22, 1982. ISSN 0581572X. URL <http://www.jstor.org/stable/25050293>.
- M.L. Rizzo and G.J. Székely. Energy distance. *WIREs Computational Statistics*, 8(1): 27–38, 2016. doi: <https://doi.org/10.1002/wics.1375>.
- Paul R Rosenbaum. An exact distribution-free test comparing two multivariate distributions based on adjacency. *Journal of the Royal Statistical Society: Series B (Statistical Methodology)*, 67(4):515–530, 2005.
- Giovanni Saraceno, Marianthi Markatou, Raktim Mukhopadhyay, and Mojgan Golzy. Goodness-of-fit and clustering of spherical data: the quadratik package in r and python, 2024. URL <https://arxiv.org/abs/2402.02290>.
- M.F. Schilling. Multivariate two-sample tests based on nearest neighbors. *Journal of the American Statistical Association*, 81(393):799–, 1986. ISSN 0162-1459.

- F.-W. Scholz and Michael A. Stephens. K-sample anderson–darling tests. *Journal of the American Statistical Association*, 82:918–924, 1987.
- A. Szabo, K. Boucher, W.L. Carroll, L.B. Klebanov, A.D. Tsodikov, and A.Y. Yakovlev. Variable selection and pattern recognition with gene expression data generated by the microarray technology. *Mathematical Biosciences*, 176(1):71–98, 2002. ISSN 0025-5564. doi: [https://doi.org/10.1016/S0025-5564\(01\)00103-1](https://doi.org/10.1016/S0025-5564(01)00103-1).
- Gábor J Székely, Maria L Rizzo, et al. Testing for equal distributions in high dimension. *InterStat*, 5(16.10):1249–1272, 2004.
- Gábor J. Székely and Maria L. Rizzo. Energy statistics: A class of statistics based on distances. *Journal of Statistical Planning and Inference*, 143(8):1249–1272, 2013. ISSN 0378-3758. doi: <https://doi.org/10.1016/j.jspi.2013.03.018>. URL <https://www.sciencedirect.com/science/article/pii/S0378375813000633>.
- A. Wald and J. Wolfowitz. On a Test Whether Two Samples are from the Same Population. *The Annals of Mathematical Statistics*, 11(2):147 – 162, 1940. doi: 10.1214/aoms/1177731909.
- Edward H. Wolf and Joseph I. Naus. Tables of critical values for a k-sample kolmogorov-smirnov test statistic. *Journal of the American Statistical Association*, 68(344):994–997, 1973.
- Yaqiong Yao and HaiYing Wang. A review on optimal subsampling methods for massive datasets. *Journal of Data Science*, 19(1):151–172, 2021. ISSN 1680-743X. doi: 10.6339/21-JDS999.
- Jin Zhang and Yuehua Wu. k-sample tests based on the likelihood ratio. *Computational Statistics and Data Analysis*, 51(9):4682–4691, 2007. ISSN 0167-9473. doi: <https://doi.org/10.1016/j.csda.2006.08.029>. URL <https://www.sciencedirect.com/science/article/pii/S0167947306002891>.